THE DYNAMICS AND CONTROL OF LARGE FLEXIBLE SPACE STRUCTURES - X

FINAL REPORT - Part I

NASA GRANT: NSG-1414, Supplement 9

by

Peter M. Bainum
Professor of Aerospace Engineering
Principal Investigator

and

A.S.S.R. Reddy
Assistant Professor
Co-Investigator

and

Feiyue Li
Cheick M. Diarra
Graduate Research Assistants

August 1987

DEPARTMENT OF MECHANICAL ENGINEERING
SCHOOL OF ENGINEERING
HOWARD UNIVERSITY
WASHINGTON, D.C. 20059

THE DYNAMICS AND CONTROL OF LARGE FLEXIBLE SPACE STRUCTURES - X

FINAL REPORT - Part I

NASA GRANT: NSG-1414, Supplement 9

by

Peter M. Bainum
Professor of Aerospace Engineering
Principal Investigator

and

A.S.S.R. Reddy
Assistant Professor
Co-Investigator

and

Feiyue Li
Cheick M. Diarra
Graduate Research Assistants

August 1987

DEPARTMENT OF MECHANICAL ENGINEERING
SCHOOL OF ENGINEERING
HOWARD UNIVERSITY
WASHINGTON, D.C. 20059

ABSTRACT

The effect of delay in the control system input on the stability of a continuously acting controller which is designed without considering the delay is studied here. The stability analysis of a second order plant is studied analytically and verified numerically. For this example it is found that the system becomes unstable for a delay which is equivalent to only 16 percent of its natural period of motion. It is also observed that even a small amount of natural damping in the system can increase the amount of delay that can be tolerated before the onset of instability. The delay problem is formulated in the discrete time domain and an analysis procedure suggested. The maximum principle from optimal control theory is applied to minimize the time required for the slewing of a general rigid spacecraft. The slewing motion need not be restricted to a single axis maneuver. The minimum slewing time is calculated based on a quasi-linearization algorithm for the resulting two point boundary value problem. Numerical examples based on the rigidized in-orbit model of the SCOLE also include the more general reflector line-of-sight slewing maneuvers.

TABLE OF CONTENTS

LIST OF FIGURES

I. INTRODUCTION

The present grant extends the research effort initiated in previous grant years (May 1977 - Feb. 1986) and reported in Refs. 1-12*. Techniques for controlling both attitude and shape of very large inherently flexible proposed future spacecraft systems are being studied. Among possible proposed future applications of these large spacecraft systems (LSS) are: Earth observation and resource sensing systems; large scale multi-beam antenna systems (e.g. for use in mobile communications); orbitally based electronic mail transmission; and as in-orbit test models designed to compare the performance of flexible LSS systems with that predicted based on computer simulations and/or scale model Earth-based laboratory experiments.

The present report is divided into two parts. This volume, designated as Part I, contains four chapters. Chapter II is based on a paper presented at the Sixth VPI&SU/AIAA Symposium on the Dynamics and Control of Large Structures which focuses on possible stability problems in LSS control systems in the presence of delayed input which has not been taken into account in the design of the closed-loop system. For the special case of a hypothetical single degree of freedom system the effect of time delay is considered both analytically and numerically. The effect of inherent (natural) damping in the system is also analyzed. The control problem with delayed input is also formulated in the discrete time domain.

*References cited in this report are listed separately at the end of each chapter.

In the following chapter the problem of minimum time attitude slewing of a general rigid spacecraft is developed based on Pontryagin's Maximum Principle. The slewing motion need not be restricted to slewing about a single axis, and the final attitude error can be made as small as required. The control torques and forces are computed and the minimum slewing time is determined using the quasilinearization algorithm for the resulting two-point-boundary value problem. Numerical examples based on the rigidized model of the Spacecraft Control Laboratory Experiment-SCOLE[13-14] include both single axis slewing as well as the more general reflector-line-of sight slewing maneuvers. (A paper based on this chapter has been accepted for presentation at the AIAA 26th Aerospace Sciences Meeting, Reno, Nevada, Jan. 1988.)

Finally Chapter IV describes the main general conclusions together with the future recommendations. The effort described here is being continued during the 1987-88 grant year in accordance with our most recent proposal.[15]

It is planned that Part II of this report will be based on the Ph.D. dissertation entitled, "On the Dynamics and Control of the Spacecraft Control Laboratory Experiment (SCOLE) Class of Offset Flexible Systems," currently being prepared by Mr. Cheick Modibo Diarra. This document will focus on the modelling, stability analysis, and control law development of the SCOLE orbiting configuration, including the effects of the mast flexibility.

References - Chapter I

1. Bainum, P.M. and Sellappan, R., "The Dynamics and Control of Large Flexible Space Structures," Final Report NASA Grant: NSG-1414, Part A: Discrete Model and Modal Control, Howard University, May 1978.

2. Bainum, Peter M., Kumar, V.K., and James, Paul K., "The Dynamics and Control of Large Flexible Space Structures," Final Report, NASA Grant: NSG-1414, Part B: Development of Continuum Model and Computer Simulation, Howard University, May 1978.

3. Bainum, P.M. and Reddy, A.S.S.R., "The Dynamics and Control of Large Flexible Space Structures II," Final Report, NASA Grant NSG-1414, Suppl. I, Part A: Shape and Orientation Control Using Point Actuators, Howard University, June 1979.

4. Bainum, P.M., James, P.K., Krishna, R., and Kumar, V.K., "The Dynamics and Control of Large Flexible Space Structures II," Final Report, NASA Grant NSG-1414, Suppl. 1, Part B: Model Development and Computer Simulation, Howard University, June 1979.

5. Bainum, P.M., Krishna, R., and James, P.K., "The Dynamics and Control of Large Flexible Space Structures III," Final Report, NASA Grant NSG-1414, Suppl. 2, Part A: Shape and Orientation Control of a Platform in Orbit Using Point Actuators, Howard University, June 1980.

6. Bainum, P.M. and Kumar, V.K., "The Dynamics and Control of Large Flexible Space Structures III," Final Report, NASA Grant NSG-1414, Suppl. 2, Part B: The Modelling, Dynamics and Stability of Large Earth Pointing Orbiting Structures, Howard University, September 1980.

7. Bainum, P.M., Kumar, V.K., Krishna, R. and Reddy, A.S.S.R., "The Dynamics and Control of Large Flexible Space Structures IV," Final Report, NASA Grant NSG-1414, Suppl. 3, NASA CR-165815, Howard University, August 1981.

8. Bainum, P.M., Reddy, A.S.S.R., Krishna, R., Diarra, C.M., and Kumar, V.K., "The Dynamics and Control of Large Flexible Space Structures V", Final Report, NASA Grant NSG-1414, Suppl. 4, NASA CR-169360, Howard University, August 1982.

9. Bainum, P.M., Reddy, A.S.S.R., Krishna, R., and Diarra, C.M., "The Dynamics and Control of Large Flexible Space Structures VI," Final Report NASA Grant NSG-1414, Suppl. 5, Howard University, Sept. 1983.

10. Bainum, P.M. Reddy, A.S.S.R., Krishna, R., Diarra, C.M. and Ananthakrishnan, S., "The Dynamics and Control of Large Flexible Space Structures-VII," Final Report NASA Grant NSG-1414, Suppl. 6, Howard University, June 1984.

11. Bainum, P.M., Reddy, A.S.S.R., Diarra, C.M. and Ananthakrishnan, S., "The Dynamics and Control of Large Flexible Space Structures- VIII," Final Report NASA Grant NSG-1414, Suppl. 7, Howard University, June 1985.

12. Bainum, P.M., Reddy, A.S.S.R., and Diarra, C.M., "The Dynamics and Control of Large Flexible Space Structures-IX," Final Report NASA Grant NSG-1414, Suppl. 8, Howard University, July 1986.

13. Taylor, L.W. and Balakrishnan, A.V., "A Mathematical Problem and a Spacecraft Control Laboratory Experiment (SCOLE) Used to Evaluate Control Laws for Flexible Spacecraft... NASA/IEEE Design Challenge," (Rev.), January 1984. (Originally presented at AIAA/VP&SU Symposium on Dynamics and Control of Large Structures, June 6-8, 1983.)

14. Proceedings of the 3rd Annual SCOLE Workshop, NASA Langley Research Center, Hampton, Va., Nov. 17-18, 1986 (compiled by Larry Taylor).

15. Bainum, P.M. and Reddy, A.S.S.R., "Proposal for Research Grant on: 'The Dynamics and Control of Large Flexible Space Structures XI,'" Howard University (submitted to NASA), October 15, 1986.

II. STABILITY ANALYSIS OF LARGE SPACE STRUCTURE CONTROL SYSTEMS WITH DELAYED INPUT

Abstract

Large space structural systems, due to their inherent flexibility and low mass to area ratio, are represented by large dimensional mathematical models. For implementation of the control laws for such systems a finite amount of time is required to evaluate the control signals; and this time delay may cause instability in the closed loop control system that was previously designed without taking the input delay into consideration. The stability analysis of a simple harmonic oscillator representing the equation of a single mode as a function of delay time is analyzed analytically and verified numerically. The effect of inherent damping on the delay is also analyzed. The control problem with delayed input is also formulated in the discrete time domain.

I. Introduction

Large flexible space structures have been proposed for possible use in communications, electronic orbital based mail systems, and solar energy collection.[1,2] The size and the low mass to area ratio of such systems warrant the consideration of the flexibility as the main contribution to the dynamics and control problem as compared to the inherently rigid nature of earlier spacecraft systems. For such large flexible systems, both orientation and surface shape control may often be required.

The equations of motion describing the shape of any large space structure are either represented by a few partial differential equations or a large number of ordinary differential equations. As the partial differential equations are difficult to solve for control system design purposes, the structural dynamics are commonly described using Finite Element Methods (FEM). Two typical large space structures namely the Hoop/Column antenna[3] and the Space Station initial operational configuration (IOC)[4] are both described using 672 degrees of freedom. Thus the dynamics of a large space structure can be written as[5]:

$$M \ddot{Z} + K Z = U_c \qquad (1)$$

where

M = NXN mass/inertia symmetric matrix

K = NXN stiffness symmetric matrix

Z = NX1 generalize coordinates representing the degrees of freedom

U_c= influence of the external forces in each degree of freedom = B'U.

With the modal transformation

$$Z = \phi\, q$$

and the properties of the modal transformation such as

$$\phi^T M \phi = I$$

$$\phi^T K \phi = \text{diag}\ [\omega_1^2\ \omega_2^2\ \ldots,\ \omega_n^2]$$

and neglecting the higher modes, equation (1) can be written in standard state space form as

$$\dot{X} = AX + BU \tag{2}$$

where

X = 2nx1 state vector representing modal coordinates and their velocities $[q, \dot{q}]^T$

U = mx1 control vector

$$A = \left[\begin{array}{c|c} 0 & I_{nxn} \\ \hline -\omega_1^2 & 0 \\ & -\omega_n^2 \end{array}\right]$$ system matrix

$$B = \left[\begin{array}{c} 0_{nxm} \\ \hline \phi^T B'_{nxm} \end{array}\right]$$ control influence matrix

II. Control with Delayed Input

The proposed control systems for large space structures are based on state variable feedback of the form:

$$U = -FX \tag{3}$$

and the control gain matrix, F, is designed using techniques such as the linear quadratic regulator (LQR) theory[6], pole placement[7], and/or linear quadratic Gaussian/loop transfer recovery (LQG/LTR).[8]

For the case when the complete state is not available for feedback, an estimate of the state, $\hat{X}$, is obtained using an appropriate estimator from the measurements of the form

$$Y = CX \tag{4}$$

where

Y = ℓx1 measurement vector

C = ℓxn sensor influence matrix

In general, it is assumed that the estimated state, $\hat{X}$, is instantaneously available. As the state estimator is implemented using a digital computer and the number of the status (2n) is of the order of hundreds for a large space structure, the computational time becomes appreciable. Thus, in the present paper, the stability of the closed loop control system, with the control as given in equation (2), is analyzed as a function of the delay time (h) using the modified control law of the form:

$$U(t) = -FX(t-h) \tag{5}$$

The characteristic equation of the closed loop system

$$\dot{X} = AX(t) - BFX(t-h) \tag{6}$$

is given by

$$G(s,h) = \det\ (sI-A+BFe^{-sh}) = 0 \tag{7}$$

which, in turn, can be written as

$$G(s,h) = \sum_{i=0}^{2n} P_i(s)e^{-shi} = 0. \tag{8}$$

The roots of the characteristic equation, (8), as a function of the delay, h, are obtained from the corresponding auxiliary equation[9]

$$G'(s,h) = \sum_{i=0}^{2n} P_i(s)(1-Ts)^{2i}\ (1+Ts)^{4n-2i} = 0 \tag{9}$$

where

$$e^{-sh} = \left[\frac{1-sT}{1+sT}\right]^2. \tag{10}$$

The value of T for which the roots of the equation (9) cross the imaginary axis in the s-plane is obtained and the corresponding h is evaluated using the relation, (10).

III. Example of a Harmonic Oscillator

The equation of motion representing the i^{th} structural mode is the familiar harmonic oscillator and is given by

$$\ddot{x}_i + \omega_i^2 x_i = f_i \tag{11}$$

Considering the delayed velocity feedback of the form

$$f_i = -2\zeta_i \omega_i \dot{x}_i \ (t-h) \tag{12}$$

with

$$\omega_i = 6, \quad \zeta_i = 0.5,$$

the characteristic equation is given by

$$G(s,h) = s^2+36+6se^{-sh} = 0 \tag{13}$$

$$= \sum_{i=0}^{1} P_i(s)e^{-shi} = 0$$

where

$$P_o(s) = s^2 + 36$$

$$P_1(s) = 6s$$

The corresponding auxilary equation is given by

$$\sum_{i=0}^{1} P_i(s) \ (1-Ts)^{2i} \ (1+TS)^{2-2i} = 0 \tag{14}$$

i.e.

$$(s^2+36) \ (1+Ts)^2 +6s(1-Ts)^2 = 0$$

or

$$T^2s^4 + (2T + 6T^2) \ s^3+(1+36T^2-12T)s^2$$

$$+ (72T+6)s+36 = 0 \tag{15}$$

Using the Routh-Hurwitz criterion, it can be found that the roots of equation (15) cross the imaginary axis at $\omega \tilde{=} 9.7$ for $T \tilde{=} 0.0426$. The corresponding delay (h) can be calculated from the relation (10) with $s = j\omega$ and is 0.16. This result can also be verified directly for this simple system with the substitution $s=j\omega$ into equation (13)[10], resulting in the value of ω and delay h for which the roots of the characteristic equation cross the imaginary axis.

Thus, equation (13) can be written as (keeping ζ_i and ω_i):

$$(\omega_i^2-\omega^2) + j(2\zeta_i\omega_i\omega)e^{-j\omega h} = 0 \tag{16}$$

or

$$(\omega_i^2-\omega^2+2\zeta_i\omega_i\omega \sin\omega h) + j2\zeta_i\omega_i\omega \cos\omega h = 0 . \tag{17}$$

For equation (17) to be satisfied

$$\cos \omega h = 0 \quad \text{or} \quad \omega h = \pi/2 \tag{18}$$

and

$$\omega_i^2-\omega^2+2\zeta_i\omega_i\omega = 0 \tag{19}$$

or $$\omega = \zeta_i\omega_i \pm \omega_i\sqrt{1+\zeta_i^2}$$

Taking the positive value for ω, the delay h, is given by

$$h = \frac{\pi/2}{\omega_i[\zeta_i+\sqrt{1+\zeta_i^2}\,]} . \tag{20}$$

The value of h for $\zeta_i = 0.5$ and $\omega_i = 6$ is 0.16 and thus the earlier result is verified. It is observed that an increase in damping reduces the tolerable delay (h) in the input.

The equation of motion of a single mode with inherent (natural) damping and velocity feedback can be written as:

$$\ddot{X}+2\zeta_i'\omega_i\dot{X}+\omega_i^2X = f = -2\zeta_i\omega_i\dot{X}(t-h) \tag{21}$$

where ζ_i' is the inherent damping ratio.

The corresponding characteristic equation is given by

$$s^2+2\zeta_i'\omega_i s+\omega_i^2+2\zeta_i\omega_i s e^{-sh} = 0 . \tag{22}$$

After substituting $s = j\omega$, equation (22) can be written as:

$$(\omega_i^2-\omega^2+2\zeta_i\omega_i\omega \sin\omega h) + j(2\zeta_i'\omega_i\omega+2\zeta_i\omega_i\omega\cos\omega h) = 0 \tag{23}$$

For equation (23) to be satisfied for all ω and h, we have

$$2\zeta_i'\omega_i+2\zeta_i\omega_i \cos\omega h = 0 \tag{24}$$

or

$$\cos \omega h = -\zeta_i'/\zeta_i \tag{25}$$

Thus, for $\cos\omega h = < 1$, the inherent damping must be less than damping due to control for instability. For $\zeta_i < \zeta_i'$, the system will always be stable.

With the value of ωh from equation (25) the frequency ω can be calculated as:

$$\omega = \omega_i \left[\sqrt{\zeta_i^2 - \zeta_i'^2} \pm \sqrt{1+\zeta_i^2 - \zeta_i'^2}\right] \tag{26}$$

and selecting the positive value of ω, h is given by:

$$h = \frac{\cos^{-1}(-\zeta_i'/\zeta_i)}{\omega_i\left[\sqrt{\zeta_i^2\zeta_i'^2} \pm \sqrt{1+\zeta_i^2\zeta_i'^2}\right]} \tag{27}$$

For $\zeta_i = \zeta'$ it can be seen that the delay, h, is half the undamped natural period of vibration. As the damping due to control increases, the tolerable delay (h) decreases and is in accordance with the observation made in the case without the inherent damping. The effect of inherent damping in the system is to increase the amount of delay that the system can tolerate without become unstable as compared to the case without damping

IV. Discrete Time Domain

As the controller is implemented on a digital computer, it may be more natural to consider the delayed input problem in the discrete time domain.

The equations of motion as given by equation (2) can be written in the discrete time domain as

$$X(i+1) = A_d X(i) + B_d U(i) \tag{28}$$

where

$$A_d = e^{A\Delta}, \quad B_d = \int_0^{\Delta} e^{A(t-\Delta)} B \, dt$$

Δ = discretization time.

The delayed input problem can be considered in discrete time in one of the two following ways:

i) Designing the controller of the form $U = -FX(i)$ without taking into consideration the delay and then examining the effect of delay on the stability of the closed-loop control system.

The control gain matrix F is designed such that the matrix $(A_d - B_d F)$ has the eigenvalues within the unit circle. Then the delay is introduced into the control law as:

$$U(i) = - FX(i-\ell) \tag{29}$$

and

$$X(i+1) = A_d X(i) - B_d F X(i-\ell) . \tag{30}$$

The stability of equation (30) can be studied using the augmented system given by

$$\underbrace{\begin{bmatrix} X(i+1) \\ X(i) \\ \\ X(i-\ell+1) \end{bmatrix}}_{\tilde{Z}(i+1)} = \underbrace{\begin{bmatrix} A_d & 0 & 0 & 0 & -B_d F \\ I & 0 & 0 & 0 & 0 \\ \\ 0 & 0 & 0 & I & 0 \end{bmatrix}}_{\tilde{A}_d} \underbrace{\begin{bmatrix} X(i) \\ X(i-1) \\ \\ X(i-\ell) \end{bmatrix}}_{\tilde{Z}(i)} \tag{31}$$

or

$$\tilde{Z}(i+1) = \tilde{A}_d \tilde{Z}(i) \tag{25}$$

(ii) Designing the control by taking into account the delay in the input.[6,11]

Equation (28) can be modified as :

$$X(i+1) = A_d X(i) + B_d U(i-\ell) \tag{32}$$

The control law of the form $U(i) = -F\tilde{Z}(i)$ can be designed from the augmented system:

$$\begin{bmatrix} X(i+1) \\ U(i) \\ U(i-1) \\ \\ U(i-\ell+1) \end{bmatrix} = \begin{bmatrix} A_d & 0 & 0 & 0 & B_d \\ 0 & 0 & 0 & 0 & 0 \\ 0 & I & 0 & 0 & 0 \\ \\ 0 & 0 & 0 & I & 0 \end{bmatrix} \underbrace{\begin{bmatrix} X(i) \\ U(i-1) \\ \\ U(i-\ell) \end{bmatrix}}_{\tilde{Z}(i)} + \begin{bmatrix} 0 \\ I \\ 0 \\ \\ 0 \end{bmatrix} U(i) \tag{33}$$

or

$$\tilde{Z}(i+1) = \tilde{A}_d Z(i) + \tilde{B}_d U(i) .$$

Thus the input $U(i-\ell)$ is a function of the previous inputs, $U(i-\ell-1)$, $U(i-\ell-2),\ldots$, and the previous states $X(i-\ell)$. Though this design can take delay into consideration, the sequence of the control signals: $U(i-\ell)$, $U(i-\ell+1),\ldots$ must be generated at an interval of one step and, thus, the original delay problem is not completely solved.

Conclusions

The effect of delay in the input on the stability of the continuous time controller that is designed without taking this delay into consideration is presented. The closed-loop control system of a second order plant becomes unstable for a delay of 0.16 seconds, which is only 16 percent of its natural period of motion. It is also observed that even a small amount of inherent (natural) damping in the system can increase the amount of delay that can be tolerated without the system becoming unstable. The delay problem is formulated in the discrete time domain and an analysis procedure is suggested.

Acknowledge

This research was supported by NASA Grant NSG-1414.

References

1. Outlook for Space, NASA Report - 386, Jan. 1976.

2. Industry Workshop on Large Space Structures, NASA CR-2709, Contract No. NAS-1-12436, for NASA LaRC, May, 1976.

3. Golden, C.T., Lackey, J.A., and Spear, E.E., "Configuration Development of the Land Mobile Satellite System (LMSS) Spacecraft," Large Space Systems Technology-1981, Third Annual Technical Review, NASA LaRC, Nov. 16-19, 1981, NASACP-2215, Part 2, pp. 711-766.

4. Housner, J.M., "Structural Dynamic Model and Response of the Deployable Reference Configuration Space Station," NASA TM86386, May 1985.

5. Bainum, Peter M., et al., "Modelling and Simulation of Dynamics and Control of Large Flexible Orbiting Systems," Journal of the Institution of Engineers (India), Vol. 66, Part 2, Aerospace Engineering, March 1986, pp. 52-56.

6. Kwakernaak, H. and Sivan, R., Linear Optimal Control Systems," Wiley, New York, 1972.

7. Kailath, T., "Linear Systems," Prentice-Hall Inc., Englewood Cliffs, N.J., 1980.

8. Doyle, J.C., and Stein, G., "Multivariable Feedback Design: Concepts for a Classical/Modern Synthesis," IEEE Trans on AC, Vol. AC-26, No. 1, Feb. 1981, pp. 4-16.

9. Thowsen, A., "An Analytic Stability Test for a class of Time Delay Systems," IEEE Trans. on AC, Vol. AC-26, No. 3, June, 1981, pp. 735-736.

10. Van Woerkom, P.Th.L.M.; Private Communication, Feb., 1986.

11. Reddy, A.S.S.R., and Gumustas, A.R., "Delay Digital Control of Large Space Structures," 13th IASTED International Conference on Modelling and Simulation, June 24-26, 1985, Lugano, Switzerland.

Appendix - Chapter II

Stability Analysis of Second Order System with Delayed State Feedback

As a second order differential equation describes the dynamics of a single mode of any large space structure, the stability analysis of such a system with delayed state feedback is analyzed and the amount of delay that can be tolerated by the system without becoming unstable is arrived at analytically.

The differential equation of second order with state feedback can be written as:

$$\ddot{x}_i + 2\zeta_i'\omega_i\dot{x}_i + \omega_i^2 x_i = -k_r x_i(t-h) - k_p \dot{x}_i(t-h) \qquad (1)$$

where

x_i = i^{th} modal coordinate

ω_i = i^{th} natural frequency

ζ_i' = i^{th} mode inherent damping ratio

k_r = rate feedback gain

k_p = position feedback gain

h = time delay

The feedback gains k_r, k_p are designed for the required stability and transient response specifications without taking the delay into consideration.

The inherent damping ratio, ζ_i' and the feedback gains, k_r and k_p; will give rise to five possible combinations as shown in Table 1 and are thus analyzed separately for mathematical convenience and easy understanding.

Case I: $\zeta_i' = 0$, $k_p = 0$ and $k_r > 0$

The differential equation of the system can be written as:

$$\ddot{x}_i + \omega_i^2 x_i = - k_r \dot{x}_i(t-h) \tag{3}$$

Case	ζ_i'	k_r	k_p
I	= 0	> 0	= 0
II	> 0	> 0	= 0
III	= 0	> 0	> 0
IV	> 0	= 0	$\neq$ 0
V	> 0	> 0	$\neq$ 0

Note: The remaining three combinations are neither feasible nor of interest.

Table 1: Feasible Combinations of ζ_i', k_r, k_p for Stability Analysis

and the corresponding characterstic equation is given by:

$$s^2 + \omega_i^2 + 2\zeta_i\omega_i s e^{-sh} = 0 \tag{4a}$$

where $k_r = 2\zeta_i\omega_i$.

The value of h for which the roots of equation (3) cross the imaginary axis can be evaluated by substituting $s = j\omega$.

Thus

$$\omega_i^2 - \omega^2 + j2\zeta_i\omega_i\omega \sin\omega h + 2\zeta_i\omega_i\omega\cos\omega h = 0 \tag{4b}$$

For equation (4b) to be satisfied

$$\sin\omega h = 0$$

and

$$\omega_i^2 - \omega^2 + 2\zeta_i\omega_i\omega \cos\omega h = 0 \tag{5}$$

Thus $\omega h = \pi/2$

and $$h = \frac{\pi/2}{\omega_i \left[\zeta_i + \sqrt{1+\zeta_i^2}\right]} \tag{6}$$

Case II: $\zeta_i' > 0$, $k_r = 2\zeta_i\omega_i$ and $k_p = 0$

The characteristic equation of the system described by equation (1) is given by

$$(\omega_i^2-\omega^2+2\zeta_i\omega_i\omega\sin\omega h) + j(2\zeta_i'\omega_i\omega+2\zeta_i\omega_i\omega\cos\omega h) = 0 \tag{7}$$

Thus $\cos\omega h = -\zeta_i'/\zeta_i$

and $$h = \frac{\cos^{-1}(\zeta_i'/\zeta_i}{\omega_i \left[\sqrt{\zeta_i^2-\zeta_i'^2} + \sqrt{1+\zeta_i^2-\zeta_i'^2}\right]} \tag{8}$$

For the case where $\zeta_i<\zeta_i'$ thesystem will always be stable since no value of h exists for which the roots of (7) cross the imaginary axis. A plot of $\omega_i h$ versus ζ_i for various values of ζ_i' is shown in Figure 2.1.

Case III: $\zeta_i' = 0$, $k_p = k_r > 0$

The characteristic equation is given by

$$s^2+\omega_i^2+k_r s e^{-sh}+k_p e^{-sh} = 0 \tag{9}$$

or $$(\omega_i^2-\omega_i^2+\omega k_r\sin\omega h+k_p\cos\omega h) + j(\omega k_r\cos\omega h-k_p\sin\omega h) = 0 \tag{10}$$

Thus $$\tan\omega h = \frac{\omega k_r}{k_p}$$

and $$\omega^2 = \frac{1}{2}\left[(2\omega_i^2+k_r^2) + \sqrt{[k_r^4+4\omega_i^2k_r^2+4k_p^2]}\right] \tag{11}$$

Plots of $h\omega_i$ versus k_r/ω_i for various values of k_p/ω_i^2 are shown in Figure 2.2. It can be seen here that these are many combinations of k_p and k_r for which the roots of Eq. (10) can cross the imaginary axis - i.e. value of $h\omega_i$ which leads to instability.

Case IV: $\zeta_i' > 0$, $k_r = 0$, $k_p \neq 0$

The characteristic equation is given by

$$(\omega_i^2-\omega^2+k_p\cos\omega h) + j(2\zeta_i'\omega_i\omega-k_p\sin\omega h) = 0 \quad (12)$$

Thus
$$\sin\omega h = \frac{2\zeta_i'\omega_i\omega}{k_p} \quad (13)$$

and
$$\omega^2 = \omega_i^2(1-2\zeta_i'^2) + \omega_i^2\sqrt{[(1-2\zeta_i'^2)^2 + (k_p/\omega_i^2)^2]} \quad (14)$$

The plots of $h\omega_i$ versus k_p/ω_1^2 for various values of ζ_i' are shown in Figure 2.3

Case V: $\zeta_i' > 0$, $k_r > 0$, $k_p \neq 0$

The characteristic equation is given by

$$(\omega_i^2-\omega^2+\omega k_r \sin\omega h+k_p\cos\omega h)$$
$$+ j(2\zeta_i' \omega_i\omega+\omega k_r\cos\omega h-k_p\sin\omega h) = 0 \quad (15)$$

By equating the imaginary part to zero, ωh can be evaluated as

$$\omega h = \sin^{-1}\underbrace{\left(\frac{2\zeta_i' \omega_i\omega}{\sqrt{k_p^2+\omega k_r^2}}\right)}_{y} - \tan^{-1}\left(\frac{\omega k_r}{k_p}\right) \quad (16)$$

after substituting ωh in the real part of equation (15), the following equation in the single unknown variable ω can be obtained

$$\omega_i^2-\omega^2+\omega k_r \sin\left(\sin^{-1}y-\tan^{-1}\left(\frac{\omega k_r}{k_p}\right)\right)$$
$$+ k_p \cos\left(\sin^{-1}y-\tan^{-1}\left(\frac{\omega k_r}{k_p}\right)\right) = 0 \quad (17)$$

Using equations (17) and (16), the limiting value for given values of ζ_i', k_r, k_p and ω_i can be determined. As the equation (17) is nonlinear, numerical procedures may have to be used and thus the generalized plots similar to the other cases may be obtained.

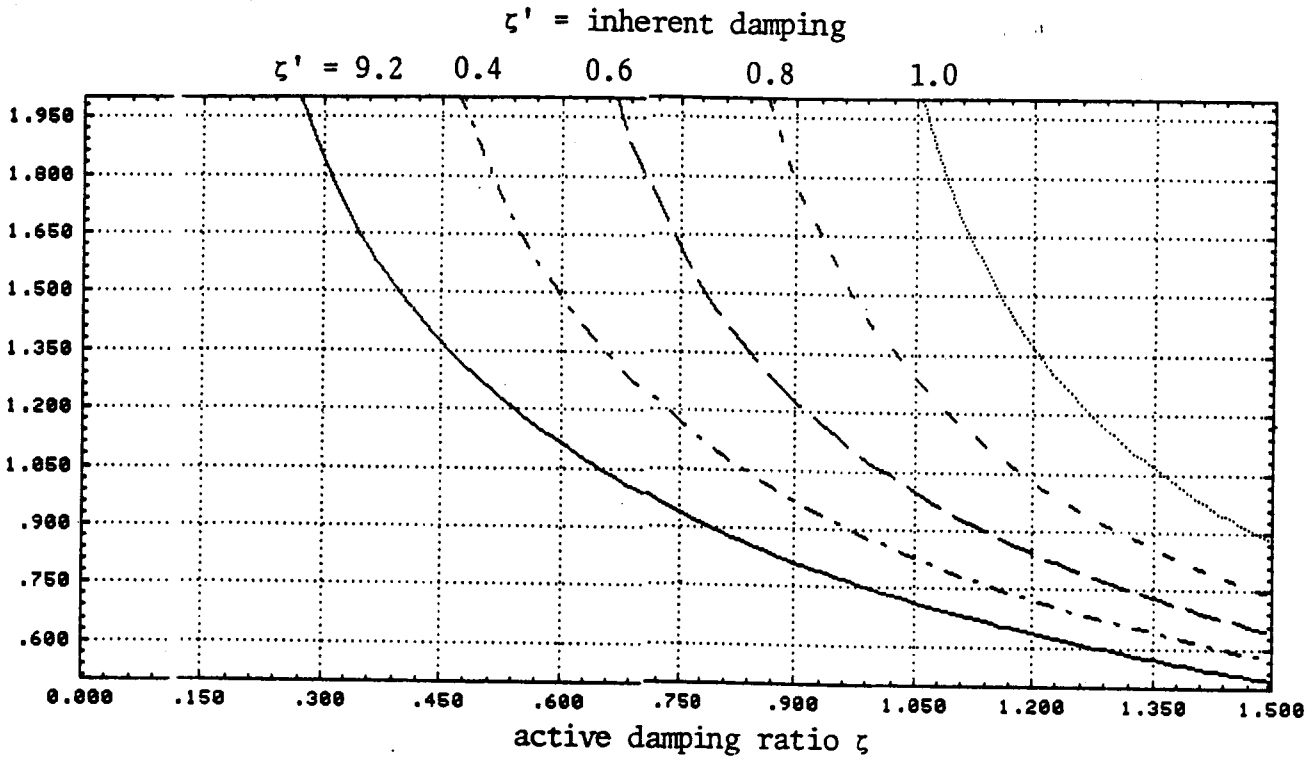

Figure 2.1: Plots of $h\omega_i$ vs ζ_i correspondence to Case II with ζ_i' as a parameter.

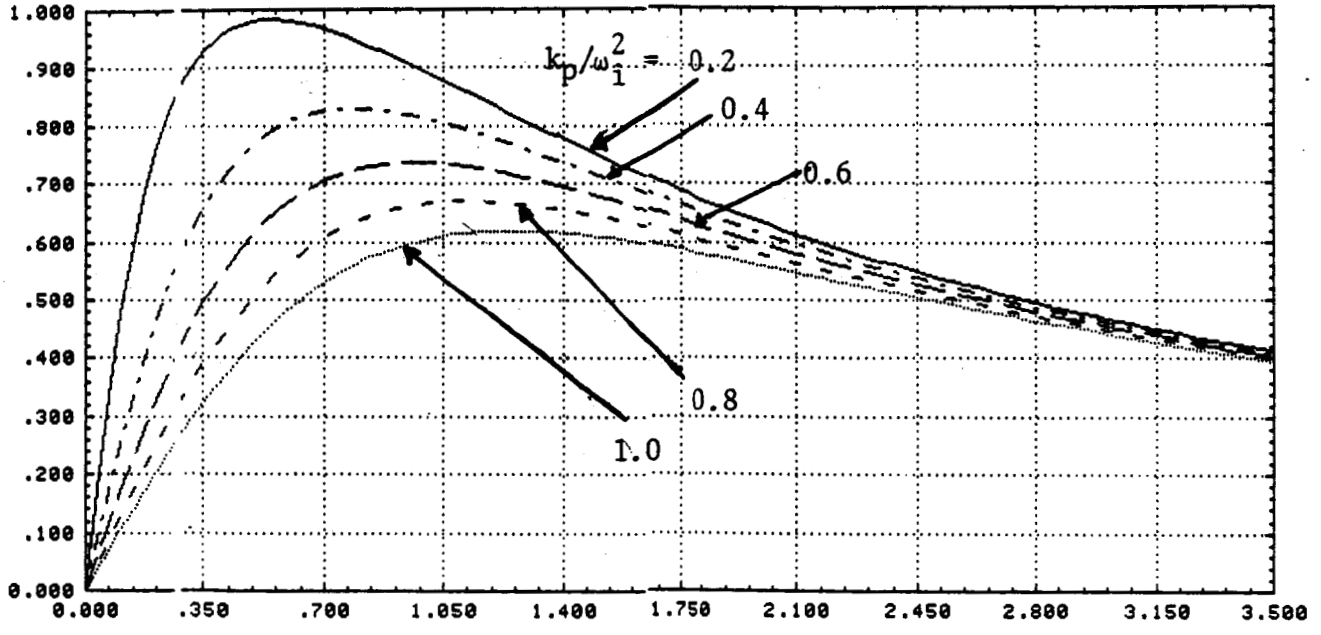

Figure 2.2 Plot of $h\omega_i$ vs k_r/ω_i corresponding to Case III with k_p/ω_i^2 as a parameter

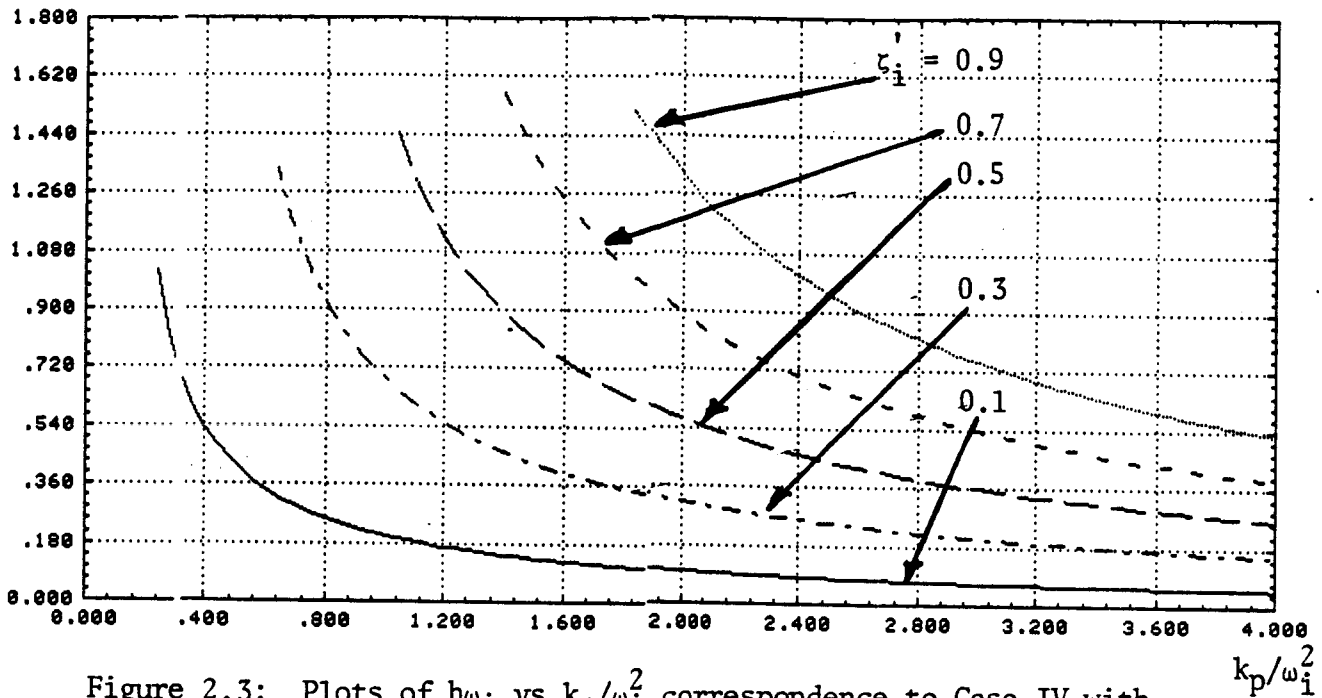

Figure 2.3: Plots of $h\omega_i$ vs k_p/ω_i^2 correspondence to Case IV with ζ_i' as a parameter

III. MINIMUM TIME ATTITUDE SLEWING MANEUVER OF A RIGID SPACECRAFT

1. Introduction

The problems of large-angle attitude maneuvers of a spacecraft have gained much consideration in recent years [1-8, 11]. In these papers, the configurations of the spacecraft considered are: (1) completely rigid, (2) a combination of rigid and flexible parts, or (3) gyrostat-type systems. The performance indices usually include minimum torque integration, power criterion, and frequency-shaped cost functionals, etc. Also some of these papers used feedback control techniques. In this paper, we try to concentrate on the minimum time slewing problem of a rigid spacecraft.

In Ref. [2], the author studied the rapid torque-limited slewing of SCOLE about a single axis (x-axis) about which the spacecraft has a small moment of inertia. The control torque about this axis is of a bang-bang type or a bang-pause-bang type. The author computed the slewing motion on the simplified model of the rigidized SCOLE [1], then worked on the practical rigidized model (with nonzero products of inertia); hence, this leads to a large error of the attitude after the slewing. Also it seems that no details were given for the controls about the other two axes (y, z).

In the present paper, we apply optimal control theory (Maximum Principle) to the slewing motion of a general rigid spacecraft (include the rigidized SCOLE, without simplification). The slewing motion need not be restricted to a single-axis slewing. The attitude error at the end of the slewing can be made as small as required. All the controls (torques and forces) are computed and the minimum slewing time is found by using the quasilinearization algorithm for the resulting two-point-boundary-value problem.

2. Attitude Description and State Equations

2.1 Attitude Description and Euler Rotation

Let $\bar{a} = [\bar{a}_1\ \bar{a}_2\ \bar{a}_3]^T$ represent a set of unit, orthogonal vectors of an inertial reference system, and $\bar{b} = [\bar{b}_1\ \bar{b}_2\ \bar{b}_3]^T$ a set of unit, orthogonal vectors of a body-fixed coordinate system of a spacecraft. Then, the attitude of the spacecraft relative to $\bar{a}$ can be described by a direction cosine matrix C with C satisfing the relation

$$\bar{b} = C\,\bar{a} \tag{1}$$

and

$$C = \begin{bmatrix} q_0^2+q_1^2-q_2^2-q_3^2 & 2(q_1q_2+q_0q_3) & 2(q_1q_3-q_0q_2) \\ 2(q_1q_2-q_0q_3) & q_0^2+q_2^2-q_3^2-q_1^2 & 2(q_2q_3+q_0q_1) \\ 2(q_1q_3+q_0q_2) & 2(q_2q_3-q_0q_1) & q_0^2+q_3^2-q_1^2-q_2^2 \end{bmatrix} \tag{2}$$

where $q=[q_0\ q_1\ q_2\ q_3]^T$ is the attitude quaternion vector and subject to a constraint equation

$$q^Tq=1 \tag{3}$$

It can be seen that q can be used not only to represent an attitude orientation of a spacecraft, but also to describe a rotation of a rigid body (spacecraft). For example, when a rigid spacecraft rotates about an axis defined by a unit vector $\varepsilon = [\varepsilon_1\ \varepsilon_2\ \varepsilon_3]^T$ fixed in both $\bar{a}$ and $\bar{b}$, the quaternion describing this rotation is

$$\begin{aligned} q_0 &= \cos(\theta/2) \\ q_i &= \varepsilon_i \sin(\theta/2) \qquad i=1,2,3 \end{aligned} \tag{4}$$

where θ is the rotation angle.

The Euler rotation theorem tells us that an arbitrary orientation of a rigid body can be accomplished by rotating it about a certain eigenaxis, $\mathcal{E} = [\mathcal{E}_1 \ \mathcal{E}_2 \ \mathcal{E}_3]^T$, through θ angle from its initial position. By means of this theorem we can find the desired rotation quaternion, q, between the initial position q(0) and the final orientation $q(t_f)$ by the relation

$$\begin{bmatrix} q_0 \\ q_1 \\ q_2 \\ q_3 \end{bmatrix} = \begin{bmatrix} q_{00} & q_{10} & q_{20} & q_{30} \\ -q_{10} & q_{00} & q_{30} & -q_{20} \\ -q_{20} & -q_{30} & q_{00} & q_{10} \\ -q_{30} & q_{20} & -q_{10} & q_{00} \end{bmatrix} \begin{bmatrix} q_{0f} \\ q_{1f} \\ q_{2f} \\ q_{3f} \end{bmatrix} \tag{5}$$

where the second subscript "$_0$" and "$_f$" represent the initial time and final time, respectively. From here, we can find $\mathcal{E}$ and θ

$$\begin{aligned} \theta &= 2 \arccos q_0 \\ \mathcal{E}_i &= q_i / \sqrt{1-q_0^2} \qquad i=1,2,3 \end{aligned} \tag{6}$$

2.1 Kinematical and Dynamical Equations

The attitude quaternion and the angular velocity of a rigid spacecraft satisfy the following kinematical and Euler dynamical equations.

$$\dot{q} = (1/2)\,\underline{\tilde{\omega}}\, q \tag{7}$$

$$I\,\dot{\omega} = \tilde{\omega}\, I\, \omega + B\, u \tag{8}$$

where

ω __ angular velocity vector in the body system, $\omega = [\omega_1\ \omega_2\ \omega_3\ ]^T$

u __ control torque and force vector, $u = [u_1\ u_2\ u_3\ \ldots\ u_n\ ]^T$

and

$$\underline{\tilde{\omega}} = \begin{bmatrix} 0 & -\omega_1 & -\omega_2 & -\omega_3 \\ \omega_1 & 0 & \omega_3 & -\omega_2 \\ \omega_2 & -\omega_3 & 0 & \omega_1 \\ \omega_3 & \omega_2 & -\omega_1 & 0 \end{bmatrix}, \qquad \tilde{\omega} = \begin{bmatrix} 0 & \omega_3 & -\omega_2 \\ -\omega_3 & 0 & \omega_1 \\ \omega_2 & -\omega_1 & 0 \end{bmatrix},$$

$$I = \begin{bmatrix} I_{11} & -I_{12} & -I_{13} \\ -I_{12} & I_{22} & -I_{23} \\ -I_{13} & -I_{23} & I_{33} \end{bmatrix},$$

and B is a 3xn alignment matrix. Eq.(8) can be rewritten, by pre-multiplying the inverse of I, as

$$\dot{\omega} = I^{-1}\,\tilde{\omega}\, I\, \omega + I^{-1}\, B\, u \tag{9}$$

The associated initial and terminal boundary conditions of the states, q, ω, are prescribed:

$$q(t=0), \quad \omega(t=0); \tag{10a}$$

$$q(t_f), \quad \omega(t_f) \tag{10b}$$

3. Optimal Control -- Two Point Boundary Value Problem

In this paper, we try to minimize the slewing time t_f,

$$t_f = \int_0^{t_f} dt \tag{11}$$

under the constraints that the elements of the control vector u have their upper and lower limits, respectively

$$u_{jmin} \leq u_j \leq u_{jmax} , \qquad j = 1,2,3, \ldots, n \tag{12}$$

Generally speaking, minimization of t_f under the constraints (12) will result in a so-called two point boundary value problem in which several controls (at least one) will reach their bounds during the slewing time, t_f. To explain this point, let us first consider a well-known special case where there are only 3 control torques, u_1, u_2, u_3, about the 3 principal axes of the spacecraft, respectively (i.e. diagonal matrix I). For this case the minimum time rotation of the spacecraft about one of its principal axes will yield the following results: the control torque about this axis is of a bang-bang type, while the other two torques remain zero. Otherwise, if the slewing motion is not about a principal axis, none of the 3 controls remain zero, but we can reason that at least one of the 3 control inputs reaches its bounds, except some jumps at the switching points during the period, t_f. As for a general case where the control torques are about a body axis system which does not coincide with the principal axes (non-diagonal I) and some additional control forces, u_4, u_5, ..., u_n, are available, the control laws become more complicated.

To handle the problem in which some controls reach their bounds and others do not, we introduce an additional cost function

$$J = \frac{1}{2} \int_0^{t_f} u^T R u \, dt \tag{13}$$

where u is the control vector, R is a proper weighting matrix. From Refs. [3] and [8], we can see that, for the case of rest-to-rest (i.e. $\omega(0)=0$, $\omega(t_f)=0$) slewing with only 3 control inputs involved, if we use only (13) as a criterion and t_f is long enough, the control torques are approximately linear functions of time, and the controls will not reach their saturation levels. But if we shorten t_f in order to find a minimum time, some of the controls must reach their bounds and, thus, contribute more effort to the slewing. By continuing the shortening of t_f, we can get a particular value, t_f^*, during which at least one of the controls remains as bang-bang with one switching point, while others are generally not of the bang-bang type. This value, t_f^*, is called the minimum time which is required.

The motivation for using (13) as our cost function are:

1) Ease of using the quasilinearization algorithm.
2) No need to determine the switching points.
3) Easy to guess the unknown initial values of the costates.

3.1 Necessary Conditions

The Hamiltonian, H, for the system (7),(9) and (13) is

$$\begin{aligned} H &= (1/2)u^T R u + p^T \dot{q} + r^T \dot{\omega} \\ &= (1/2)u^T R u + (1/2)p^T \tilde{\omega} q + r^T (I^{-1} \tilde{\omega} I \omega + I^{-1} B u) \end{aligned} \tag{14}$$

where p and r are costate vectors associated with q and ω,

$$p = [p_0 \; p_1 \; p_2 \; p_3]^T, \quad r = [r_1 \; r_2 \; r_3]^T.$$

By means of the maximum principle, the necessary conditions for minimizing J, are

$$\dot{p} = -(\partial H/\partial q) \;, \quad ==> \quad \dot{p} = (1/2)\,\tilde{\omega}\, p \tag{15}$$

$$\dot{r} = -(\partial H/\partial \omega) \;, \quad ==> \quad \dot{r} = g(\omega, r) + (1/2)[q]p \tag{16}$$

where $g(\omega, r)$ is a 3x1 vector function of ω and r, and the detailed form of $g(\omega, r)$ can be found in Appendix I; [q] is a 3x4 matrix

$$[\,q\,] = \begin{bmatrix} q_1 & -q_0 & -q_3 & q_2 \\ q_2 & q_3 & -q_0 & -q_1 \\ q_3 & -q_2 & q_1 & -q_0 \end{bmatrix}$$

The initial values of p, r are unknown, p(t=0), r(t=0).

If u is a 3x1 control torque vector and B is a 3x3 nonsingular matrix, R can be a positive-definite matrix defined by

$$R = B^T B \tag{17}$$

From

$$\frac{\partial H}{\partial u} = 0 \;, \quad ==> \quad R\,u + B^T I^{-1} r = 0$$

$$\text{or} \quad u = -R^{-1} B^T I^{-1} r$$

$$= -B^{-1} I^{-1} r \tag{18}$$

we have

$$u_j = \begin{cases} u_{jmin}, & \text{if } u_j < u_{jmin}; \\ -(B^{-1} I^{-1} r)_j, & \text{if } u_{jmin} \le u_j \le u_{jmax}; \\ u_{jmax}, & \text{if } u_j > u_{jmax}. \end{cases} \tag{19}$$

$$j=1,2,3.$$

If u is an nx1 (n>3) vector, B is a 3xn matrix, the R formed by (17) is a semi-positive-definite matrix. To circumvent the singularity of R, we introduce a 3x1 vector, v,

$$v = B\,u \tag{20}$$

Then

$$(\partial H/\partial v) = 0 \ , \quad ==> \quad v = -I^{-1} r \tag{21}$$

By means of pseudo-inverse of matrix B, B^+, we can get u

$$u = B^+ v = B^T(BB^T)^{-1} v$$

$$= - B^T(BB^T)^{-1}(I^{-1}r) \tag{22}$$

The control laws are

$$u_j = \begin{cases} u_{jmin}, & \text{if } u_j < u_{jmin}; \\ -(B^+ I^{-1} r)_j, & \text{if } u_{jmin} \le u_j \le u_{jmax}; \\ u_{jmax}, & \text{if } u_j > u_{jmax}. \end{cases} \tag{23}$$

$$j=1,2, \ldots, n.$$

Note that Eq.(23) is reduced to Eq.(19) if B^{-1} exists.

In summary, we seek the function q(t), ω(t), u(t), p(t), and r(t) which satify the equations (7), (9), (15-16), (23) subject to the boundary contions (10).

3.2 Properties of the initial values of p

The key to settle this problem is to find the unknown initial values of the costates

$$p(0)=[\ p_{00}\ p_{10}\ p_{20}\ p_{30}\ ]^T \text{ and } r(0)=[\ r_{10}\ r_{20}\ r_{30}]^T$$

Notice that the coefficient matrix of the right side of Eq.(15) is anti-symmetric, so,

$$p^T\dot{p} = 0$$

$$\text{i.e.} \quad p^Tp = \text{constant}$$

The extra constant is usually treated as an unknown and is determined by iteration. This results in more computational effort. However, as we shall prove, this unknown constant can be easily selected without changes in the optimal controls [8].

Compare Eqs.(7) and (15), they have the same coefficient matrix on the right sides. Therefore, they have the same state transition matrix. Let Q represent this 4x4 matrix, then the q and p at any instant can be obtained by

$$q = Q\, q(0) \ , \qquad p = Q\, p(0) \tag{24}$$

We know that Q satisfies the following matrix differential equation

$$\dot{Q} = (1/2)\, \tilde{\underline{\omega}}\, Q \tag{25}$$

Ref. [10] shows that Q, the solution of (25), has the form

$$Q = \begin{bmatrix} q_{11} & -q_{12} & -q_{13} & -q_{14} \\ q_{12} & q_{11} & q_{14} & -q_{13} \\ q_{13} & -q_{14} & q_{11} & q_{12} \\ q_{14} & q_{13} & -q_{12} & q_{11} \end{bmatrix} \tag{26}$$

On substituting Eq.(26) into Eq.(25) we can verify that only 4 of the 16 q_{ij} are independent. We rewrite the first equation of (24) as

$$\begin{bmatrix} q_0 \\ q_1 \\ q_2 \\ q_3 \end{bmatrix} = \begin{bmatrix} q_{00} & -q_{10} & -q_{20} & -q_{30} \\ q_{10} & q_{00} & -q_{30} & q_{20} \\ q_{20} & q_{30} & q_{00} & -q_{10} \\ q_{30} & -q_{20} & q_{10} & q_{00} \end{bmatrix} \begin{bmatrix} q_{11} \\ q_{12} \\ q_{13} \\ q_{14} \end{bmatrix} \tag{27}$$

where $q_{00}=q_0(0)$, $q_{10}=q_1(0)$, etc. It is clear that the coefficient matrix of Eq.(27) is orthogonal, so

$$\begin{bmatrix} q_{11} \\ q_{12} \\ q_{13} \\ q_{14} \end{bmatrix} = \begin{bmatrix} q_{00} & q_{10} & q_{20} & q_{30} \\ -q_{10} & q_{00} & q_{30} & -q_{20} \\ -q_{20} & -q_{30} & q_{00} & q_{10} \\ -q_{30} & q_{20} & -q_{10} & q_{00} \end{bmatrix} \begin{bmatrix} q_0 \\ q_1 \\ q_2 \\ q_3 \end{bmatrix} \tag{28}$$

From Eq.(28) we get

$$q_{11}^2 + q_{12}^2 + q_{13}^2 + q_{14}^2 = 1$$

This means that Q is also orthogonal. On the other hand, we have a similar equation for p,

$$\begin{bmatrix} p_0 \\ p_1 \\ p_2 \\ p_3 \end{bmatrix} = \begin{bmatrix} p_{00} & -p_{10} & -p_{20} & -p_{30} \\ p_{10} & p_{00} & -p_{30} & p_{20} \\ p_{20} & p_{30} & p_{00} & -p_{10} \\ p_{30} & -p_{20} & p_{10} & p_{00} \end{bmatrix} \begin{bmatrix} q_{11} \\ q_{12} \\ q_{13} \\ q_{14} \end{bmatrix} \tag{29}$$

After substituting Eq.(28) into Eq.(29) and eliminating q_{11}, q_{12}, q_{13}, q_{14}, one arrives at

$$\begin{bmatrix} p_0 \\ p_1 \\ p_2 \\ p_3 \end{bmatrix} = \begin{bmatrix} d_0 & -d_1 & -d_2 & -d_3 \\ d_1 & d_0 & -d_3 & d_2 \\ d_2 & d_3 & d_0 & -d_1 \\ d_3 & -d_2 & d_1 & d_0 \end{bmatrix} \begin{bmatrix} q_0 \\ q_1 \\ q_2 \\ q_3 \end{bmatrix} \tag{30}$$

where the constants d_0, d_1, d_2, d_3, are given by

$$\begin{bmatrix} d_0 \\ d_1 \\ d_2 \\ d_3 \end{bmatrix} = \begin{bmatrix} q_{00} & q_{10} & q_{20} & q_{30} \\ -q_{10} & q_{00} & -q_{30} & q_{20} \\ -q_{20} & q_{30} & q_{00} & -q_{10} \\ -q_{30} & -q_{20} & q_{10} & q_{00} \end{bmatrix} \begin{bmatrix} p_{00} \\ p_{10} \\ p_{20} \\ p_{30} \end{bmatrix} \tag{31}$$

Eq.(30) represents the relationship between the quaternion and the associated costates. Eq.(30) can be rewritten as

$$\begin{bmatrix} p_0 \\ p_1 \\ p_2 \\ p_3 \end{bmatrix} = \begin{bmatrix} q_0 & -q_1 & -q_2 & -q_3 \\ q_1 & q_0 & q_3 & -q_2 \\ q_2 & -q_3 & q_0 & q_1 \\ q_3 & q_2 & -q_1 & q_0 \end{bmatrix} \begin{bmatrix} d_0 \\ d_1 \\ d_2 \\ d_3 \end{bmatrix} \tag{32}$$

Substituting of Eq.(32) into Eq.(16) results in

$$\dot{r} = g(\omega, r) + \begin{bmatrix} q_1 & -q_0 & -q_3 & q_2 \\ q_2 & q_3 & -q_0 & -q_1 \\ q_3 & -q_2 & q_1 & -q_0 \end{bmatrix} \begin{bmatrix} q_0 & -q_1 & -q_2 & -q_3 \\ q_1 & q_0 & q_3 & -q_2 \\ q_2 & -q_3 & q_0 & q_1 \\ q_3 & q_2 & -q_1 & q_0 \end{bmatrix} \begin{bmatrix} d_0 \\ d_1 \\ d_2 \\ d_3 \end{bmatrix}$$

or

$$\dot{r} = g(\omega, r) - \frac{1}{2} \begin{bmatrix} 0 & q_0^2+q_1^2-q_2^2-q_3^2 & 2(q_1q_2+q_0q_3) & 2(q_1q_3-q_0q_2) \\ 0 & 2(q_1q_2-q_0q_3) & q_0^2+q_2^2-q_3^2-q_1^2 & 2(q_2q_3+q_0q_1) \\ 0 & 2(q_1q_3+q_0q_2) & 2(q_2q_3-q_0q_1) & q_0^2+q_3^2-q_1^2-q_2^2 \end{bmatrix} \begin{bmatrix} d_0 \\ d_1 \\ d2 \\ d3 \end{bmatrix}$$

or

$$\dot{r} = g(\omega, r) - (1/2)\, C\, d \tag{33}$$

where $d=[d_1\ d_2\ d_3]^T$, C is just the attitude matrix given by Eq.(2). It can be seen that r is independent of d_0, from Eq.(33), and u depends only on r, from Eq.(23). Therefore, u is also independent of d_0. This means the arbitrary selection of the value of d_0 yields the same extremum control, u. Now we can explain the results in Ref.[11]. In view of Eq.(31), we have

$$d_0^2 + d_1^2 + d_2^2 + d_3^2 = p_{00}^2 + p_{10}^2 + p_{20}^2 + p_{30}^2 \tag{34}$$

If we set $d_0=0$ the norm of the initial costates in Eq.(34) reaches its minimum, the solution of which is considered in Ref. [3]. From Eq.(31) we can also know that $d_0=0$ means

$$p(0)^T q(0)=0$$

4. Initial Values of Costates and the Slewing Time

By means of Euler's eigenaxis rotation theorem, from the known attitudes at the initial and final time, $q(0)$ and $q(t_f)$, we can find a unit vector (eigenaxis), $\mathcal{E}$, which is fixed in both the body axes and inertial coordinate system, and a rotation angle, θ^*. Then the attitude changes from $q(0)$ to $q(t_f)$ can be realized by rotating the spacecraft about the axis, $\mathcal{E}$, through the angle, θ^*.

Theoretically, there are many ways through which we can change the attitude from its initial value, $q(0)$, to its final value, $q(t_f)$. For example, this change of attitude can be achieved by successively rotating the spacecraft about the x, y, z axes (i.e. 1-2-3 rotations) through certain displacements in the angles, θ_1, θ_2, θ_3, respectively. To do this way, we need to speed up (and slow down) the spacecraft 3 times, and the total rotation angle is, $\theta_1+ \theta_2+ \theta_3$. On the other hand, for the Euler rotation, we only need to rotate the spacecraft about $\mathcal{E}$ once through the angle θ^* which is less than the total angle required by any other way. Since the Euler rotation is simple and requires a smaller angle, it may take less time and consume less energy (torques and forces). Therefore, in view of our cost functions, (11) and (13), it is reasonable to think that the optimal slewing is near the Euler rotation. We shall call this rotation the "expected rotation", which is determined only from the initial and final attitude of the spacecraft and will be used in obtaining a set of approximate unknown initial values of the costates and the starting solution of the quasilinearization algorithm.

4.1 Initial Values of Costates

Before starting the quasilinearization algorithm, we need to

guess the unknown initial values of the costates, p and r. Considering the analytical solution about a single principal axis maneuver in Ref. [3], we define a rotation angle $\theta(t)$, about an arbitrary axis $\mathcal{E}$,

$$\theta(t)=\theta(0)+\dot{\theta}(0)t+\frac{1}{2}\ddot{\theta}(0)t^2+\frac{1}{6}\dddot{\theta}(0)t^3 \tag{35}$$

where $\theta(0)$, $\dot{\theta}(0)$, $\ddot{\theta}(0)$, $\dddot{\theta}(0)$ are constants to be determined.

For simplicity, here we only consider the solution of θ with the following boundary conditions

$$\theta(0)=0, \quad \dot{\theta}(0)\neq 0, \quad \theta(t_f)=\theta^* \quad \dot{\theta}(t_f)=0 \tag{36}$$

These conditions correspond to the boundary conditions of the states

$$q(0), \quad \omega(0)\neq 0, \quad q(t_f), \quad \omega(t_f)=0$$

Substituting Eq.(36) into Eq.(35) yields

$$\ddot{\theta}(0)=(6\theta^*/t_f^2)-(4\dot{\theta}(0)/t_f) \tag{37a}$$

$$\dddot{\theta}(0)=-(12\theta^*/t_f^3)+(6\dot{\theta}(0)/t_f^2) \tag{37b}$$

For the Euler's rotation, the angular velocity and its derivatives are expressed as follows

$$\omega=\mathcal{E}\dot{\theta}, \quad \dot{\omega}=\mathcal{E}\ddot{\theta}, \quad \ddot{\omega}=\mathcal{E}\dddot{\theta} \tag{38}$$

To approximately determine the initial values of p and r, we need to use the dynamical Eqs.(9) and (33). Upon using Eqs.(20) and (21), substituting v (u) into Eq.(9) and solving for r, we get

$$r = I\,\tilde{\omega}\,I\omega - I^2\dot{\omega} \tag{39}$$

and the derivatives

$$\dot{r}=\frac{d}{dt}(I\,\tilde{\omega}\,I\omega)-I^2\ddot{\omega} \tag{40}$$

At the same time, from Eq.(33), and noting that $C^T=C^{-1}$,

$$d = 2\,C^T\,[\,g(\omega, r)-\dot{r}\,] \tag{41}$$

At the time t=0, by putting Eqs.(37-38) into Eqs.(39-41), we can get the approximate values of r(0) and d. As for p(0), we can set $P_0(0)=0$ (since d_0 can be arbitrarily chosen) and solve for d_0 and $P_i(0)$, i=1, 2,3, by using Eq.(32).

Now we determine $\dot{\theta}(0)$ from known initial value $\omega(0)$. Generally, $\omega(0)$ is not equal to $\mathcal{E}\dot{\theta}$ because $\mathcal{E}$ is independent of $\omega(0)$. Let e be the difference between them

$$e = \mathcal{E}\dot{\theta}(0) - \omega(0)$$

To find a minimum value of e^Te, we differentiate e^Te with respect to $\dot{\theta}(0)$ and note that $\mathcal{E}^T\mathcal{E}=1$, we get

$$\dot{\theta}(0) = \mathcal{E}^T\omega(0) \tag{42}$$

By using the initial values p(0) and r(0) obtained above, and integrating the differential equations (7), (9), (15-16), with Bu in Eq.(9) replaced by v in Eqs.(20) and (21), we can get a set of values, q(t), ω(t), p(t), and r(t), $0 \leq t \leq t_f$, which will be used as the starting values of the quasilinearization method.

4.2 Initial Value of t_f

The starting value $t_f^{(0)}$ needs to be made as close to the minimum time, t_f^*, as possible. This can be done by using the techniques similar to those described above. Suppose the slewing motion is an Euler rotation about a vector, $\mathcal{E}$, through an angle, θ(t). Then, by putting the first two equations of Eq.(38) and Eq.(20) into Eq.(8), we get

$$I\,\mathcal{E}\,\ddot{\theta} = \dot{\theta}^2\,\tilde{\mathcal{E}}\,I\,\mathcal{E} + v \tag{43}$$

For simplicity, we only consider the case $v_{imin}=-v_{imax}$. Then, let $c_i=v_{imax}$ and $v_i=c_i\tau_i$; the above vector equation can be expressed as the following 3 similar equations for θ(t):

$$a_i \ddot{\theta} = b_i \dot{\theta}^2 + c_i \tau_i \qquad i = 1,2,3 \qquad (44)$$

where a_i, b_i, and c_i are constants, τ_i is the normalized control about the ith body axis and

$$|\tau_i| \leq 1 \qquad i=1,2,3 \qquad (45)$$

Each equation of Eq.(44) with the boundary condition Eq.(36) can be treated as a minimum time control problem with the constraint (45). It is easy to see that the control for this problem is of a bang-bang type and the problem can be solved analytically to get the minimum time t^*_{fi} (i=1, 2, 3) as functions of θ^* and $\dot{\theta}(0)$. The results are shown in Appendix II.

Since the only minimum time, t_f^*, that every equation of Eq.(44) can accept at the same time is the longest one, we use the largest one as our initial guess for t_f.

4.3 The Quasilinearization Algorithm[9]

We choose the quasilinearization algorithm to solve the two point boundary value problem because this method needs only to solve linear differential equations and it converges quadratically.

Let $z=[q_0\ q_1\ q_2\ q_3\ w_1\ w_2\ w_3\ p_0\ p_1\ p_2\ p_3\ r_1\ r_2\ r_3]^T$, then Eqs.(7), (9),(15-16) can be replaced by

$$\dot{z} = f(z,u) \qquad (46)$$

with the boundary conditions

$$z_i(0) = L_i \qquad i=1,2,\cdots,8 \qquad (47a)$$

$$z_j(t_f) = M_j \qquad j=1,2,\cdots,7 \qquad (47b)$$

The 8th initial condition is $z_8(0)=p_0(0)$ (arbitrarily chosen).

Suppose that at the Nth stage of the iteration, an approximate solution reasonably close to the exact solution has been obtained.

Then, the linearized form of Eq.(46) at the (N+1)st stage of the iteration about the nominal functions, which are the solution obtained at the Nth stage of the iteration, is

$$\dot{z} = (\partial f/\partial z)(z^{(N)},u^{(N)})\ (z^{(N+1)}-z^{(N)}) + (\partial f/\partial u)(z^{(N)},u^{(N)})\ (u^{(N+1)}-u^{(N)}) + f(z^{(N)},u^{(N)}) \quad (48)$$

where $\partial f/\partial z$ and $\partial f/\partial u$ are the gradient matrices evaluated at $z^{(N)}$, and $u^{(N)}$. The $u^{(N+1)}$ in Eq.(48) is determined as follows. At a point on the optimal trajectory, it is assumed that $u^{(N)}$ satifies Eq.(23). If for some j (j=1,2, $\cdots$, n), $u^{(N)}_j = u_{jmax}$ (or u_{jmin}), then

$$u^{(N+1)}_j = u^{(N)}_j \quad (49)$$

On the other hand, the linearized form of Eq.(23) is

$$u^{(N+1)}-u^{(N)} = - B^{+}I^{-1}(r^{(N+1)}-r^{(N)}) \quad (50)$$

For $i \neq j$ (i=1,2, $\cdots$,n),

$$u^{(N)}_i = -(B^{+}I^{-1}r^{(N)})_i$$

By putting this equation into Eq.(50), we have

$$u^{(N+1)}_i = -(B^{+}I^{-1}r^{(N+1)})_i \quad (51)$$

Replacing $u^{(N+1)}$ in Eq.(48) by Eq.(49) and Eq.(51), we can get a linear differential equation for $z^{(N+1)}$

$$\dot{z}^{(N+1)} = A(z^{(N)},u^{(N)})z^{(N+1)} + D(z^{(N)},u^{(N)}) \quad (52)$$

which is nonhomogeneous and subject to the boundary conditions (47):

$$z^{(N)}_i(0) = z_i(0) = L_i, \quad i=1,2, \cdots, 8 \quad (53a)$$

$$z^{(N)}_j(t_f) = z_j(t_f) = M_j, \quad j=1,2, \cdots, 7 \quad (53b)$$

and can be solved using the method of particular solutions.

Let $y_1, y_2, \ldots, y_6$ represent the solutions of Eq.(52) with the following initial conditions

$$y_1(0)=[L_1\ L_2\ \cdots\ L_8\ 1\ 0\ 0\ \cdots\ 0]^T$$

$$y_2(0)=[L_1\ L_2\ \cdots\ L_8\ 0\ 1\ 0\ \cdots\ 0]^T$$

$$\vdots \qquad\qquad \vdots$$

$$y_6(0)=[L_1\ L_2\ \cdots\ L_8\ 0\ 0\ \cdots\ 0\ 1]^T$$

Let y_7 be the solution of Eq.(52) with the initial condition

$$y_7(0)=[L_1\ L_2\ \cdots\ L_8\ 0\ 0\ \cdots\ 0\ 0]^T$$

We now have 7 particular solutions of Eq.(52), $y_1(t)$, $y_2(t)$, $\cdots$, $y_7(t)$, $0 \le t \le t_f$. The general solution of Eq.(52) can be written as a linear combination of these particular solutions

$$z = B_1y_1 + B_2y_2 + \cdots + B_6y_6 + B_7y_7 \tag{54}$$

where $B=[B_1\ B_2\ \cdots\ B_7]^T$ are constants to be determined and subject to

$$B_1+B_2+\cdots+B_7=1 \tag{55}$$

By letting the components z_2, $\cdots$, z_7 satisfy the final conditions (53b), we get

$$\begin{bmatrix} y_{12} & y_{22} & \cdots & y_{72} \\ \vdots & \vdots & \cdots & \vdots \\ y_{17} & y_{27} & \cdots & y_{77} \end{bmatrix} \begin{bmatrix} B_1 \\ \vdots \\ B_7 \end{bmatrix} = \begin{bmatrix} M_2 \\ \vdots \\ M_7 \end{bmatrix} \tag{56}$$

Note that $z_1=q_0$ is related to q_1, q_2, q_3 according to Eq.(3) We solve Eqs.(55-56), and eliminate B_7, to get

$$[B_1\ B_2\ \cdots\ B6]^T=[p_{10}^{(N+1)}\ p_{10}^{(N+1)}\ p_{10}^{(N+1)}\ r_0^{(N+1)}]^T$$

To summarize the above results, we have a step by step description of the quasilinearization algorithm:

(a) Obtain nominal function, $z^{(0)}(t)$, and the slewing time $t^{(0)}_f$ discussed in sections 4.1 and 4.2.

(b) At the (N+1)st stage of the iteration (N=1,2, $\cdots$) determine whether the components of the control vector are on their

bounds (have maximum admissible amplitudes) at any point in $[0, t_f^{(k)}]$ using the conditions in Eq.(23) .Evaluate the matrix A and vector D of Eq.(52) in $[0, t_f^{(k)}]$.

(c) Solve the linear two-point boundary-value problem, Eq.(52), using the method of particular solutions. Obtain the function $z^{(N+1)}(t)$. Compute the function $u^{(N+1)}(t)$ from Eqs. (49) and (51).

(d) Compute

$$\rho = \max\left\{ \left| p_{i0}^{(N+1)} - p_{i0}^{(N)} \right|, \left| r_{j0}^{(N+1)} - r_{j0}^{(N)} \right| \ , \ i,j = 1,2,3 \right\}$$

$$\text{if } \left| p_{i0}^{(N+1)} \right| \leq 1 \text{ and } \left| r_{j0}^{(N+1)} \right| \leq 1 \ ;$$

or

$$\rho = \max\left\{ \frac{\left| p_{i0}^{(N+1)} - p_{i0}^{(N)} \right|}{\left| p_{j0}^{(N+1)} \right|}, \frac{\left| r_{j0}^{(N+1)} - r_{j0}^{(N)} \right|}{\left| r_{j0}^{(N+1)} \right|} \ , \ i,j = 1,2,3 \right\}$$

$$\text{if } \left| p_{i0}^{(N+1)} \right| > 1 \text{ and } \left| r_{j0}^{(N+1)} \right| > 1 \ .$$

(e) If $\rho < \delta$, a small preselected positive quantity, the optimal solution for $t_f^{(k)}$ is obtained. Then go to (f). Otherwise, go to (b) and the iterated solution is used as the nominal function for the next stage of the iteration (N=N+1).

(f) If one of the controls is of a bang-bang type, stop computation, and the $t_f^{(k)}$ is the minimum time t_f^*. If not, shorten $t_f^{(k)}$ to $t_f^{(k+1)}$ by a reasonable amount and go to (b).

5. Numerical Results

Finally, we apply these methods described in the previous sections to the SCOLE slewing motion[1]. Fig. 1 shows the configuration of the SCOLE. It is composed of a Space Shuttle and a large reflecting antenna. The antenna is attached to the Shuttle by a flexible beam. Since we only consider the motion of the rigid SCOLE in this paper, the flexibility of the beam is ignored. The X, Y, Z axes are the spacecraft axes corresponding to roll, pitch and yaw axes, respectively. The controls considered in this paper include three moments about the X, Y, Z axes of the system and two forces applied at the center of the reflector in the X, Y directions only. The inertia parameters of the SCOLE and the saturation levels of the controls are listed in Table 1.

Table 1. Inertia Parameters and Limits of Controls

I_{11}=1,132,508	I_{22}=7,007,447	I_{33}=7,113,962	SLUG
I_{12}=- 7,555	I_{23}= 115,202	I_{31}= 52,293	-FT^2
u_1 $u_{xmax} = -u_{xmin}$			
u_2 $u_{ymax} = -u_{ymin}$	= 10,000		FT-LB
u_3 $u_{zmax} = -u_{zmin}$			
u_4 $f_{xmax} = -f_{xmin}$	= 800		LB
u_5 $f_{ymax} = -f_{ymin}$			

The associated alignment matrix B is

$$B = \begin{bmatrix} 1 & 0 & 0 & 0 & 130 \\ 0 & 1 & 0 & -130 & 0 \\ 0 & 0 & 1 & 32.5 & 18.75 \end{bmatrix}$$

We have done some numerical simulations for the following cases:

(a) A diagonal inertia matrix I is used. The control is assumed to be provided only by torques on the Shuttle. No control forces on the reflector are assumed. The expected rotation is a rotation about one of the three principal axes, through 20 deg., from rest to rest. The result is exactly the same as that of the theoretical analysis discussed earlier in this paper, i.e., the control torque about the slewing axis is of a bang-bang type while the others remain zero.

(b) Extend the inertia matrix in case (a) to a non-diagonal form. The expected rotation is a rotation about one of the three spacecraft axes and the rotation angle is 20 deg.

Fig.2 and Fig.3 give the control torques for the expected rotations "X- axis slewing" and "Z-axis slewing", respectively. Fig.2 shows that u_x is near of a bang-bang type, while u_y, u_z are not. The non-zero contributions of the u_y and u_z are due to the offset of the inertia distribution of the SCOLE configuration (non-diagonal matrix I). Similar situations are shown in Fig.3 where u_z is near to a bang-bang type and others are not.

The starting value of $t^{(0)}_f$ for these slewings (X- and Z- axes) are $t^{(0)}_f$=12.5749 sec. and $t^{(0)}_f$=31.5166 sec., respectively, by using the method in section 4.2. The minimum time, t^*_f, we actually obtained are t^*_f=12.57 sec. and t^*_f=31.33 sec., respectively. These results indicate that the estimated values for t^*_f are very accurate.

Fig. 4 shows the changes of attitude angles O_x, O_y, O_z (1-2-3 Euler angles) for the "X-axis slewing" of Fig.2. The O_x changes from zero to 20 deg., but O_y and O_z change very little during the slewing and finally approach zero. The non-zero changes in O_y and O_z are also

due to the offset of the structural distribution of the SCOLE.

Fig.5 shows the attitude changes for the "Z-axis slewing" (Fig.3) Unlike the case in Fig. 4, the Ox changes greatly. This change is due to the unsymmetrical moments of inertia about the X-axis and Y-axis.

Fig. 6 shows the control torques for the "X-axis slewing" with a slewing time t_f=15.37 sec., which is 2.8 sec. more than the minimum time t^*_f=12.57 sec.(Fig. 2). The controls are almost linear functions of time (rest-to-rest slewing). u_x is less than the saturation level, and u_y, u_z are near zero. From Fig.6 and Fig.2, we see that much more control effort (approximate 50%) is saved if we increase the slewing time a little. Another feature of using a longer slewing time in the computation is that it needs less number (4 times) of iterations for convergence than by using a minimum slewing time t^*_f (12 times). These properties suggest that, in practical applications of this problem, it is not necessary to seek the minimum time, t^*_f, and the associated extremum controls. It is enough to know approximate values of the t^*_f and the controls.

(c) Following the case (b), we now add two control force actuactors on the reflector, f_x and f_y. Figs. 7a, 7b and Fig. 8 show the control torques, forces and attitude angles for the "X-axis slewing" motion. The slewing time t^*_f is greatly shortened, t^*_f=3.988 sec. (about one third of the slewing time without the forces f_x and f_y).

Figs. 9-14 show the controls and attitude angle changes for the "z-axis slewing". For the sake of comparison, we use 3 different t_f in the computation, t_f=27.5 sec., t_f=26.1 sec. and t^*_f=20.0 sec. (minimum time; recall that t^*_f=31.33 sec. without f_x and f_y). From Figs. 9-11, the control torques approach the bang-bang type, and the maximum

amplitude of the control forces increases gradually. From Fig. 12 to Fig. 14, we can see the obvious increases in θ_x and θ_y. This is due to the increases in u_x, u_y, f_x and f_y.

(d) Now we consider a general case. Suppose the SCOLE is in an Earth orbit and we need the line of sight to be directed toward the center of the Earth. The orbital coordinate system (x, y, z) is shown in the following figure.

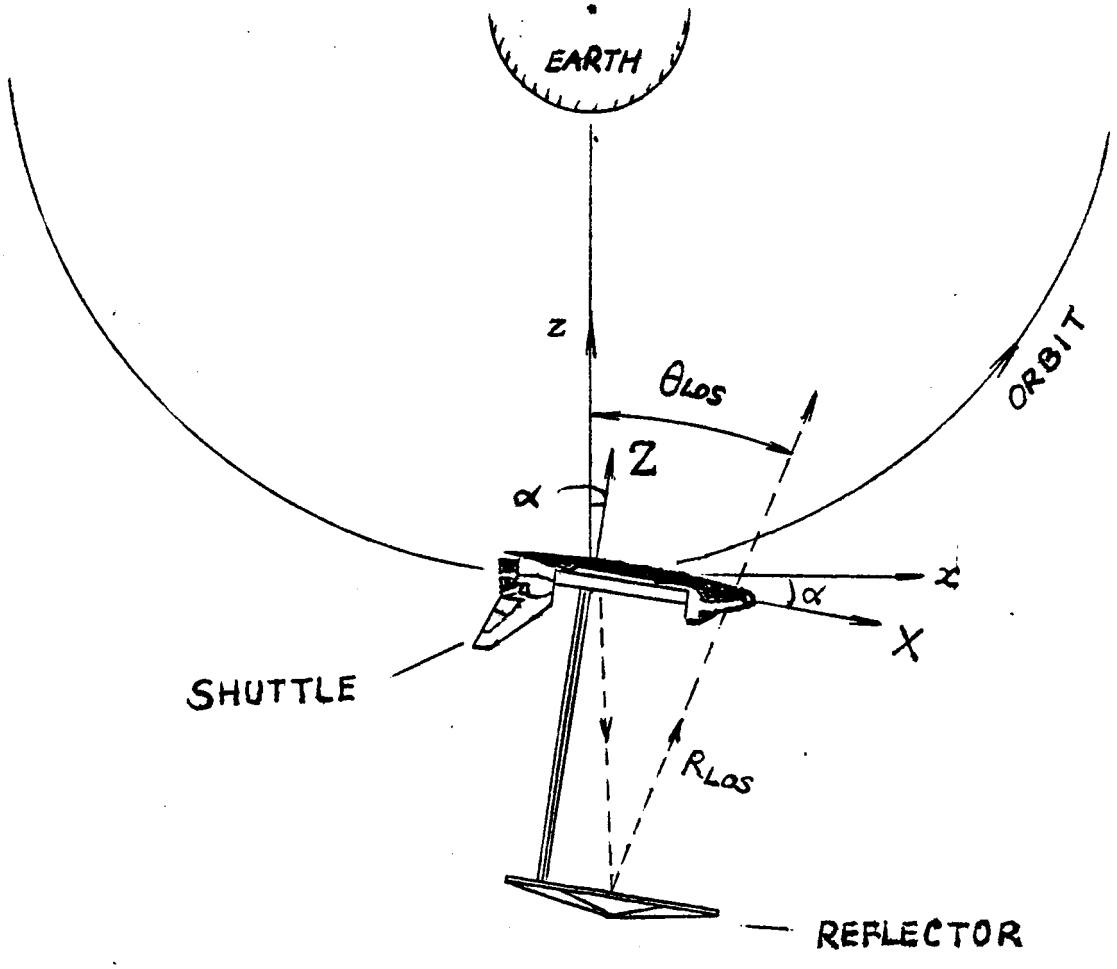

ATTITUDE OF THE SCOLE

Suppose, before the slewing, the Y axis of the spacecraft coincides with the orbital y axis, and the angle difference between x and X (or z and Z) axes is α=7.897224212 deg. Thus the initial attitude quaternion of the spacecraft is

$$q_0(0) = \cos(\alpha/2)$$

$$q_2(0) = \sin(\alpha/2) \ , \ q_1(0)=q_3(0)=0$$

According to Ref.[1], the unit vector along the line of sight in the rigid SCOLE coordinate system is

$$\hat{R}_{LOS} = \begin{bmatrix} 0.1112447155 \\ -0.2410302170 \\ 0.9641208678 \end{bmatrix}$$

The direction cosines of the orbital z axis in the body system at the initial time are represented by

$$\hat{z}_{/B} = \begin{bmatrix} \sin\alpha \\ 0 \\ \cos\alpha \end{bmatrix}$$

Therefore the angle between $\hat{R}_{LOS}$ and $\hat{z}_{/B}$ at the initial time is

$$\theta_{LOS}(0) = \hat{R}_{LOS} \cdot \hat{z}_{/B} = 0.9641208678 \cos\alpha - 0.1112447155 \sin\alpha$$

$$= 20 \text{ deg.}$$

The eigen axis of the expected rotation in the body system is determined by

$$\epsilon = \frac{\hat{R}_{LOS} \times \hat{z}_{/B}}{|\hat{R}_{LOS} \times \hat{z}_{/B}|}$$

Thus the quaternion for this rotation is

$$q_0 = \cos(20^\circ/2)$$

$$q_i = \epsilon_i \sin(20^\circ/2) \ , \ i=1,2,3$$

From Eq.(5) we can get the final attitude quaternion, $q(t_f)$.

Figs. 15a and 15b show the control torques (without the reflector control forces) and attitude angles for this slewing motion.

The guessed starting value of t_f is $t_f^{(0)}$=26.3482 sec. and the actually converged value of t_f is t_f^*=25.01 sec. The O_{LOS} in Fig. 15b is the angle between the line of sight and the line of the target direction (from the spacecraft to the center of the Earth).

Conclusion Remarks

(1) There is a good agreement between the guessed value of t_f and the value of t_f to which the algorithm converges in the cases (b) and (d).

(2) The guessed initial values of the costates here: p(0), r(0) are adequate for the algorithm to converge. If the slewing time, t_f, is sufficiently larger than the minimum time, t_f^*, then, the converged values of p(0) and r(0) are very close to the guessed values and less number (4 times) of iterations is needed (Fig. 6). The same situation was observed in Ref. 8.

(3) The control profiles obtained in this paper give us a good reference for future use. For example, an extension to the minimum time slewing motion of the SCOLE model containing both rigid and flexible components is planned.

References

[1]. Taylor, L.W. and Balakrishnan, A.V., "A Mathematical Problem and a Spacecraft Control Laboratory Experiment (SCOLE) used to Evaluate Control Laws for Flexible Spacecraft ...NASA/IEEE Design Challenge," Jan., 1984.

[2]. Lin, J.G., "Rapid Torque-Limited Line-of-sight Pointing of SCOLE (Spacecraft Control Laboratory Experiment) Configuration," AIAA/AAS Astrodynamics Conference, Williamsburg, Va., August, 1986, AIAA paper 86-1991.

[3]. Junkins, J.L. and Turner, J.D., "Optimal Continuous Torque Attitude Maneuvers," Journal of Guidance and Control, Vol. 3, No. 3, May-June, 1980, pp. 210-217.

[4]. Skaar, S.B. and Kraige, L.G., "Large-Angle Spacecraft Attitude Maneuvers Using an Optimal Reaction Wheel Power Criterion," The Journal of the Astronautical Sciences, Vol. 32, No. 1, Jan.-March 1984, pp. 47-61.

[5]. Chen, J. and Kane, T.R., "Slewing Maneuvers of Gyrostart Spacecraft." The Journal of the Astronautical Sciences, Vol. 28, No. 3, July-Sept. 1980, pp. 267-281.

[6]. Turner, J.D. and Junkins, J.L., "Optimal Large-Angle Single-Axis Rotational Maneuvers of Flexible Spacecraft, Journal of Guidance and Control, Vol. 3, No. 6, Nov-Dec. 1980, pp. 578-585.

[7]. Chun, H.M. and Turner, J.D., "Frequency-Shaped Large-Angle Maneuvers," AIAA 25th Aerospace Sciences Meeting, Jan. 12-15, 1987, Reno, Nevada, AIAA paper 87-0174.

[8]. Bainum, P.M. and Feiyue Li, "Optimal Torque Control SCOLE Slewing Maneuvers," 3rd Annual SCOLE Workshop, Nov. 17, 1986, NASA Langley Research Center, Hampton, Virginia.

[9]. Yeo, B.P., Waldron, K.J. and Goh, B.S., "Optimal Initial Choice of Multipliers in the Quasilinearization Method for Optimal Control Problems with Bounded Controls," Int. J. Control, 1974, Vol. 20, No. 1, pp. 17-33.

[10]. Morton, H.S. Jr., Junkins, J.L. and Balnton, J.N., "Analytical Solutions for Euler Parameters", Celestial Mechanics, Vol. 10, No. 3, 1974, pp. 287-301.

[11]. Vadali, S.R., Kraige, L.G. and Junkins, J.L., "New Results on the Optimal Spacecraft Attitude Maneuver Problem", J. Guidance and Control, Vol. 7, No. 3, May-June, 1984, pp. 378-380.

Figure 1. Drawing of the Shuttle/Antenna Configuration.

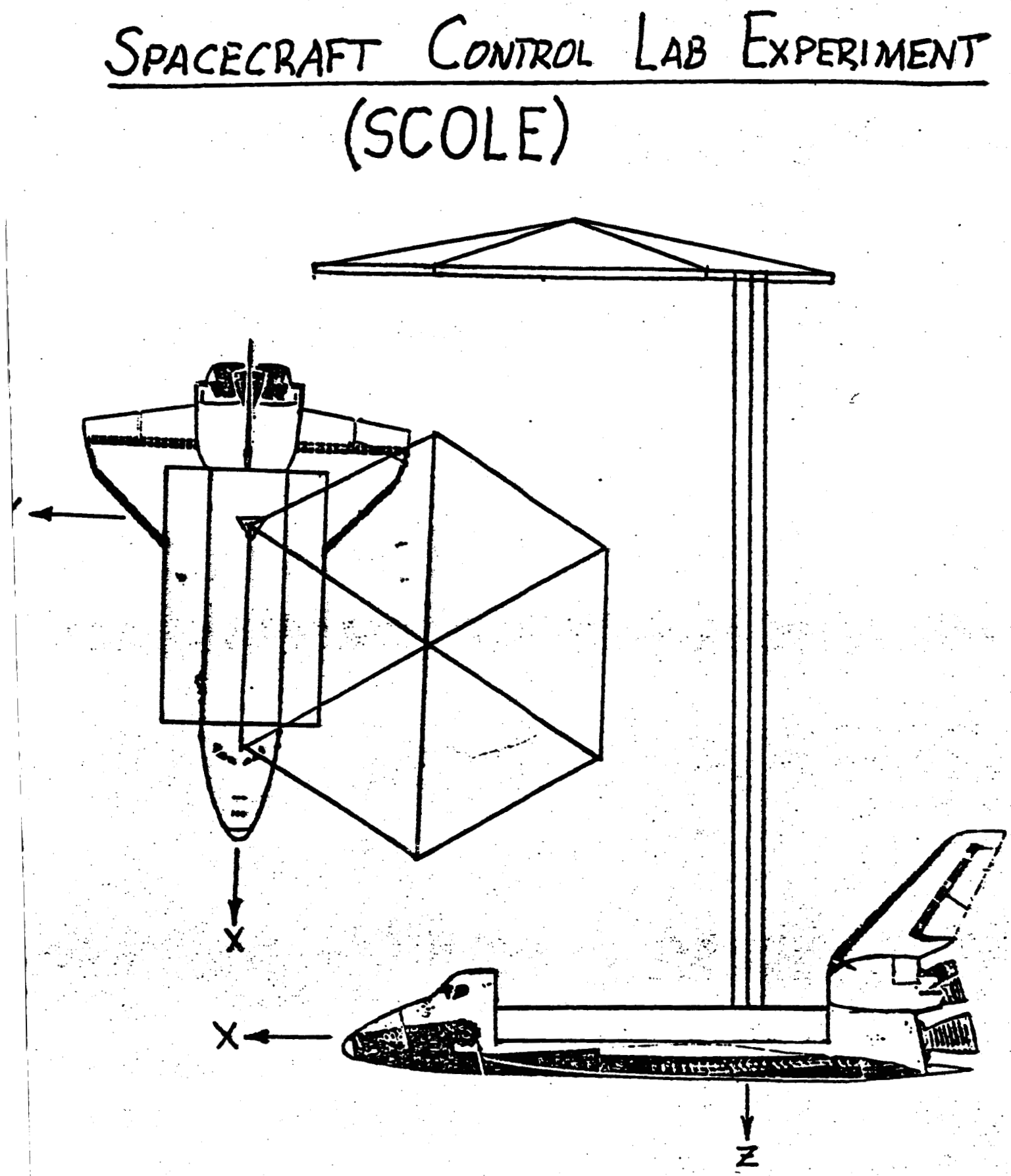

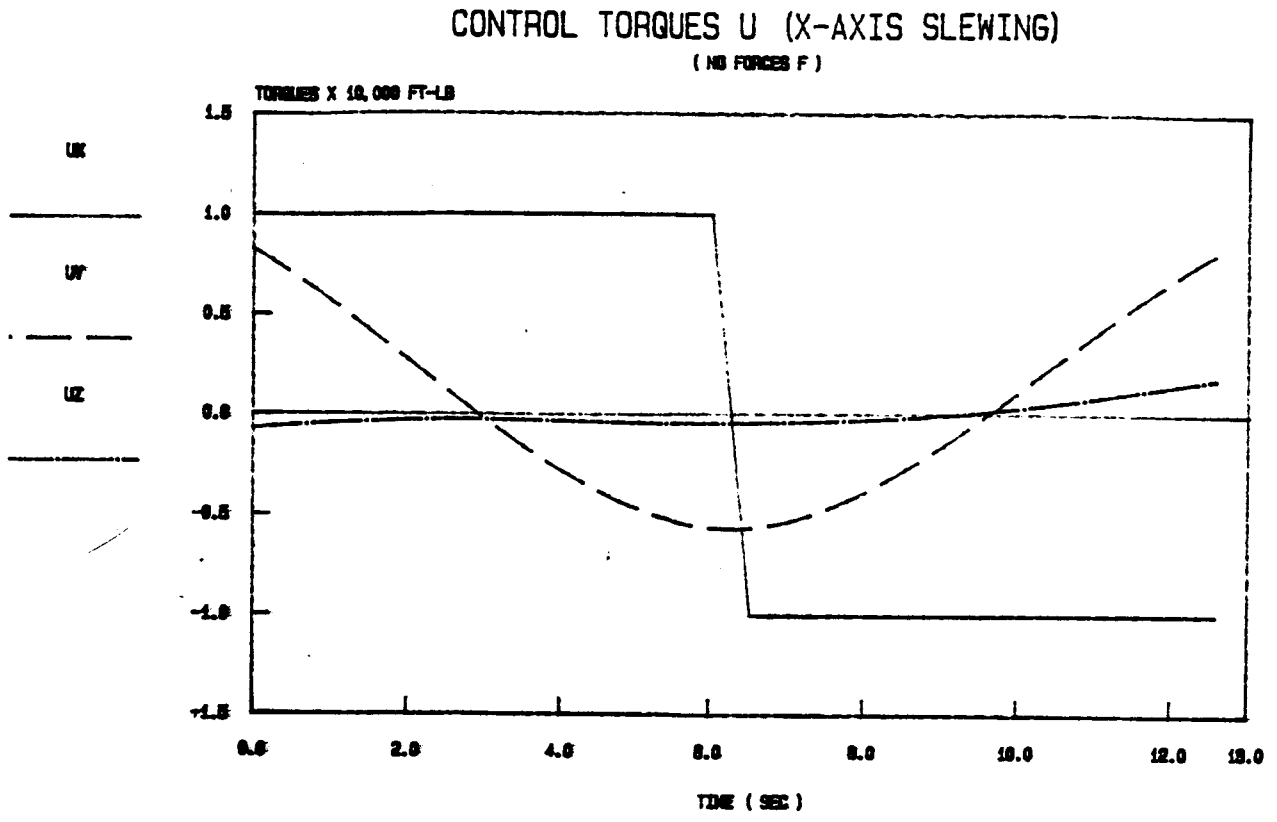
CONTROL TORQUES U (X-AXIS SLEWING)
(NO FORCES F)
TORQUES X 10,000 FT-LB
UX
UY
UZ
1.5
1.0
0.5
0.0
-0.5
-1.0
-1.5
0.0
2.0
4.0
6.0
8.0
10.0
12.0
13.0
TIME (SEC)

Fig. 2

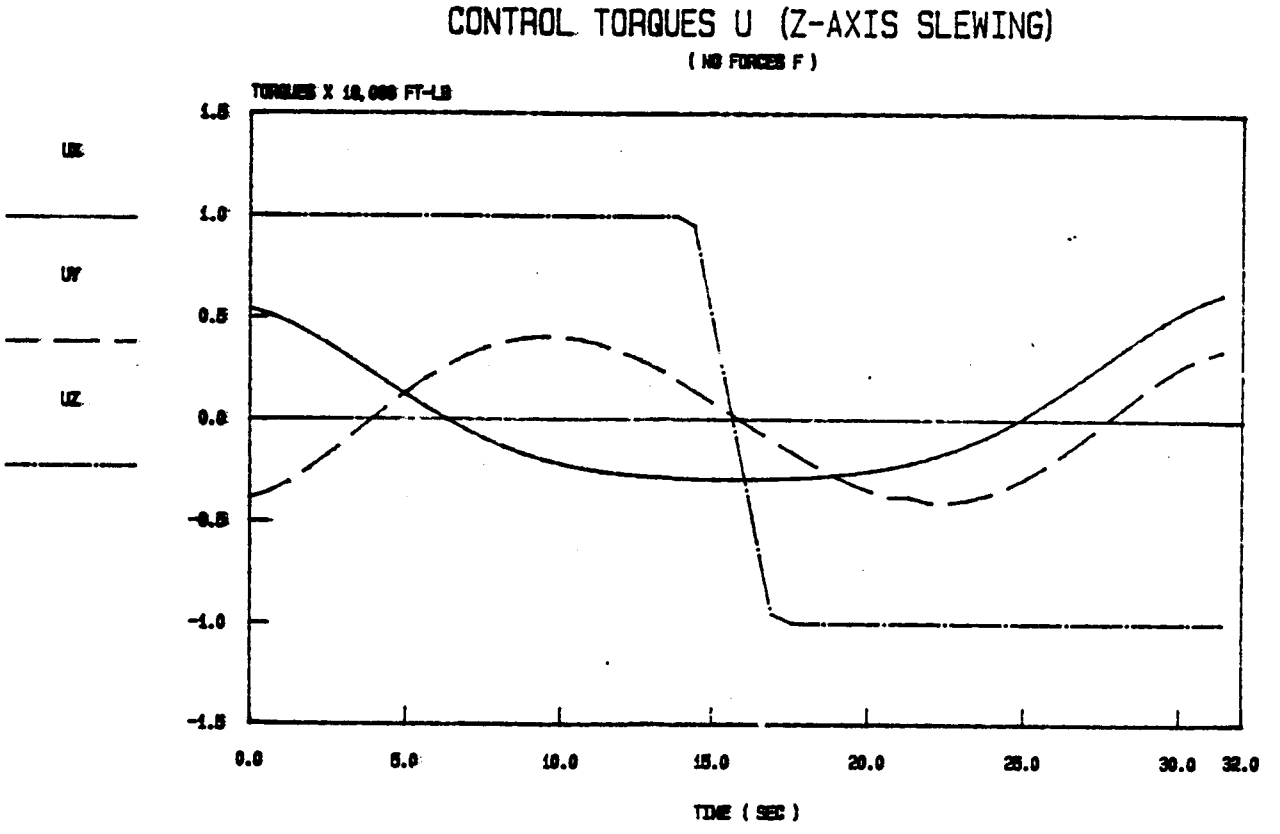
CONTROL TORQUES U (Z-AXIS SLEWING)
(NO FORCES F)
TORQUES X 10,000 FT-LB
UX
UY
UZ
1.5
1.0
0.5
0.0
-0.5
-1.0
-1.5
0.0
5.0
10.0
15.0
20.0
25.0
30.0
32.0
TIME (SEC)

Fig. 3

ATTITUDE ANGLES (X-AXIS SLEWING)

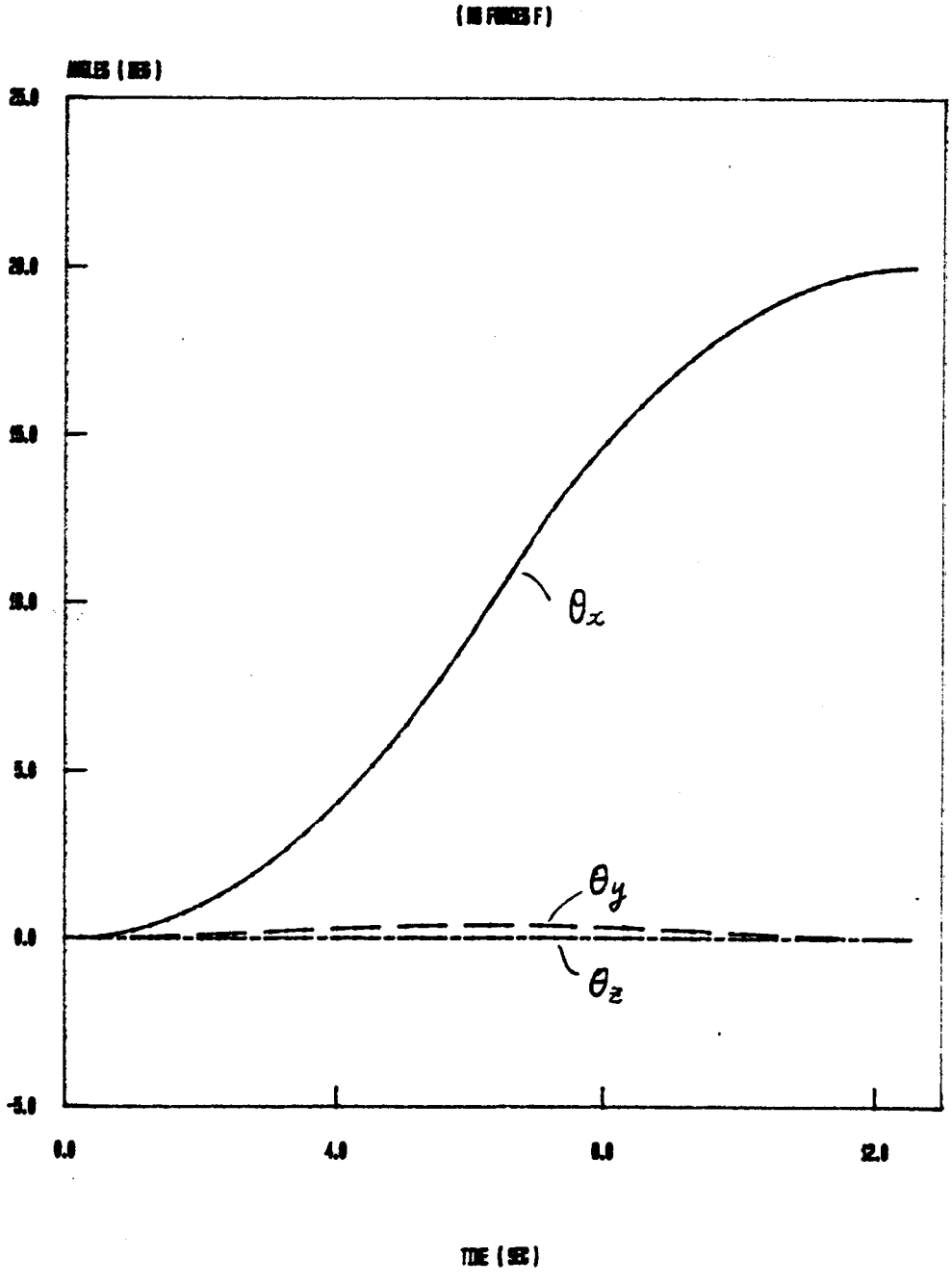

Fig. 4

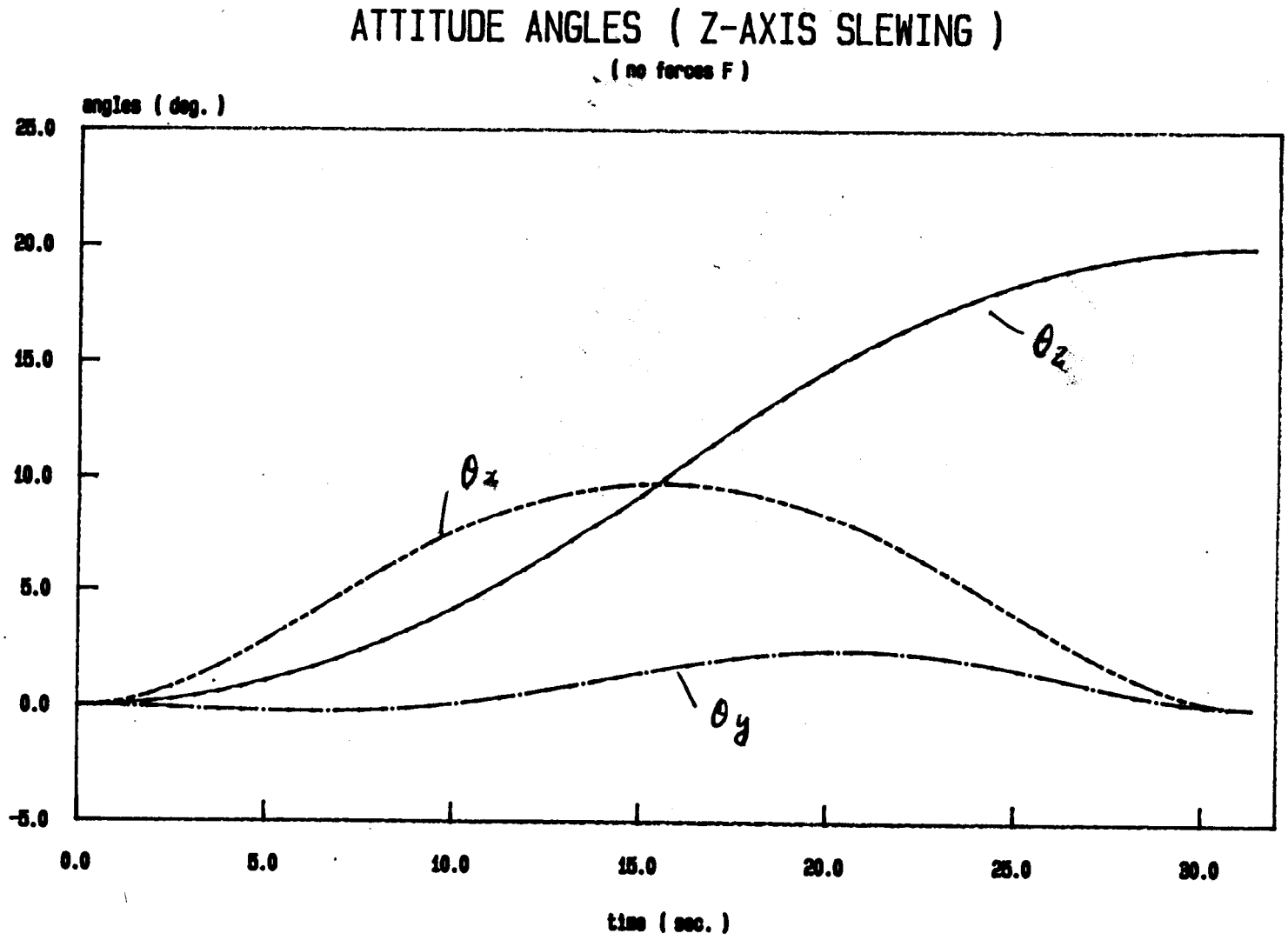
ATTITUDE ANGLES (Z-AXIS SLEWING)
(no forces F)
angles (deg.)
25.0
20.0
15.0
10.0
5.0
0.0
-5.0
0.0
5.0
10.0
15.0
20.0
25.0
30.0
time (sec.)
θz
θx
θy

Fig. 5

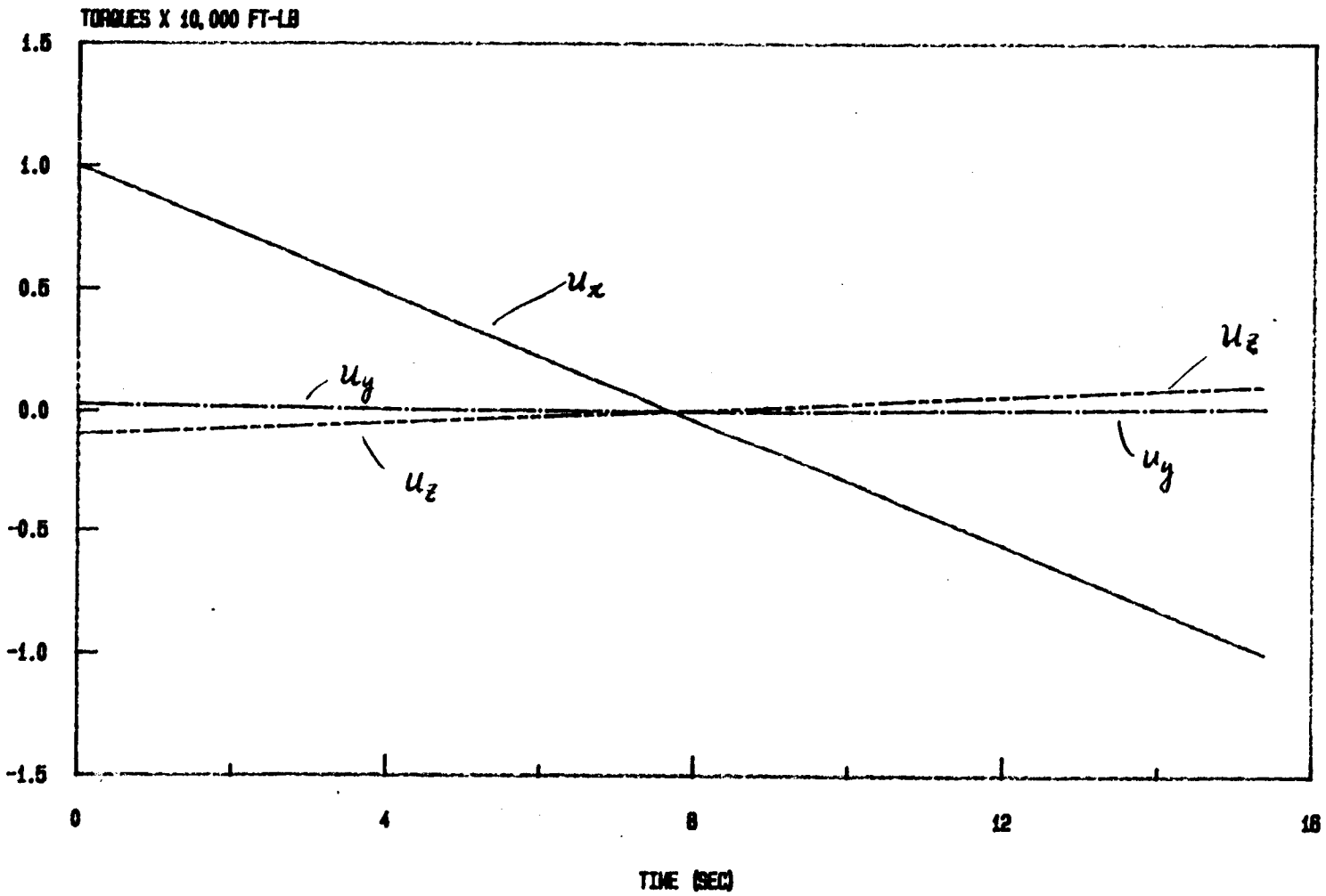
CONTROL TORQUES (X-AXIS SLEWING)
(NO FORCES F)
TORQUES X 10,000 FT-LB
1.5
1.0
0.5
0.0
-0.5
-1.0
-1.5
0
4
8
12
16
TIME (SEC)
u_x
u_y
u_z
u_z
u_y

Fig. 6

Fig. 7a CONTROL TORQUES U (X-AXIS SLEWING)

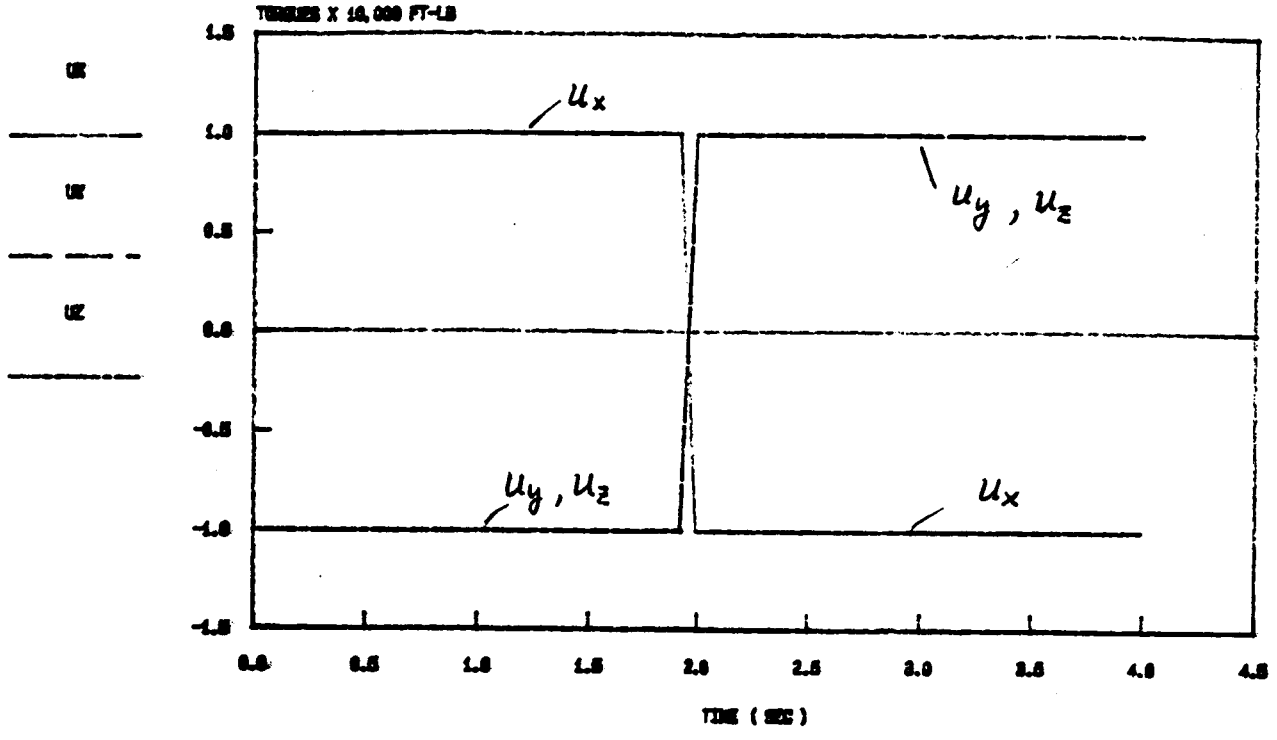

Fig. 7b CONTROL FORCES F (X-AXIS SLEWING)

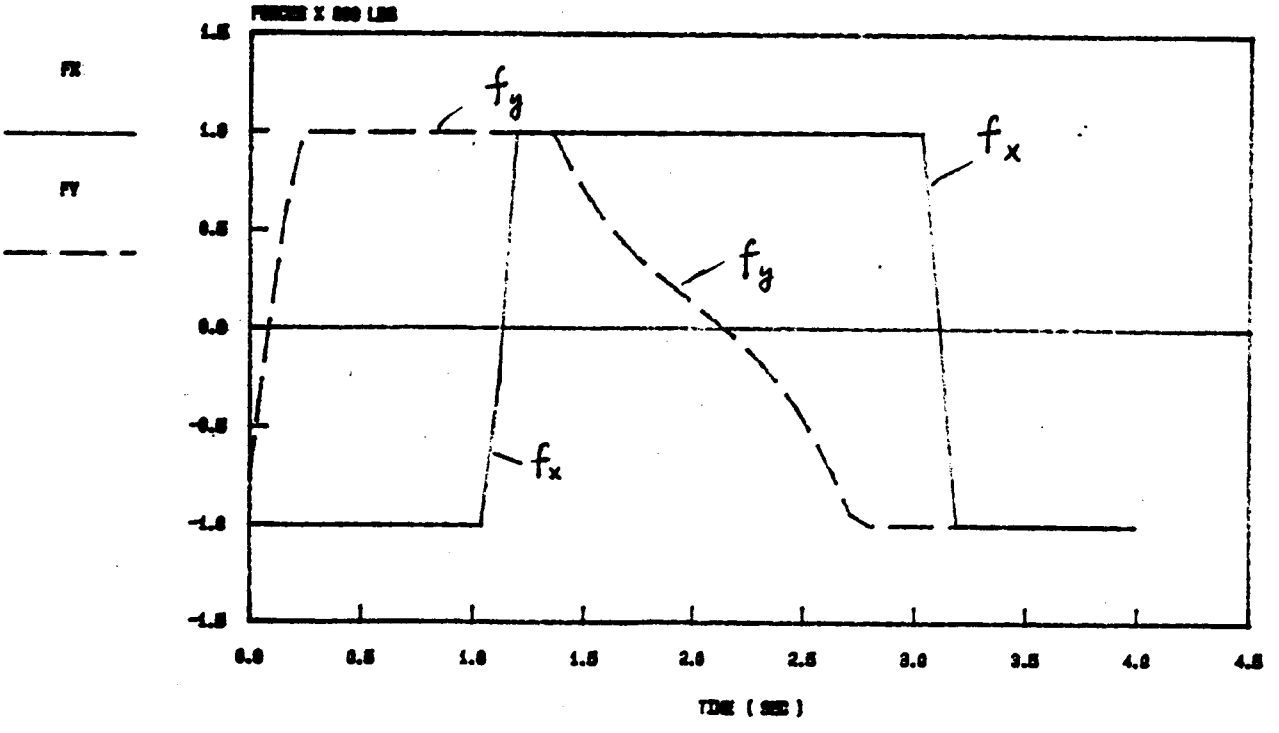

Fig. 8 ATTITUDE ANGLES (X-AXIS SLEWING)

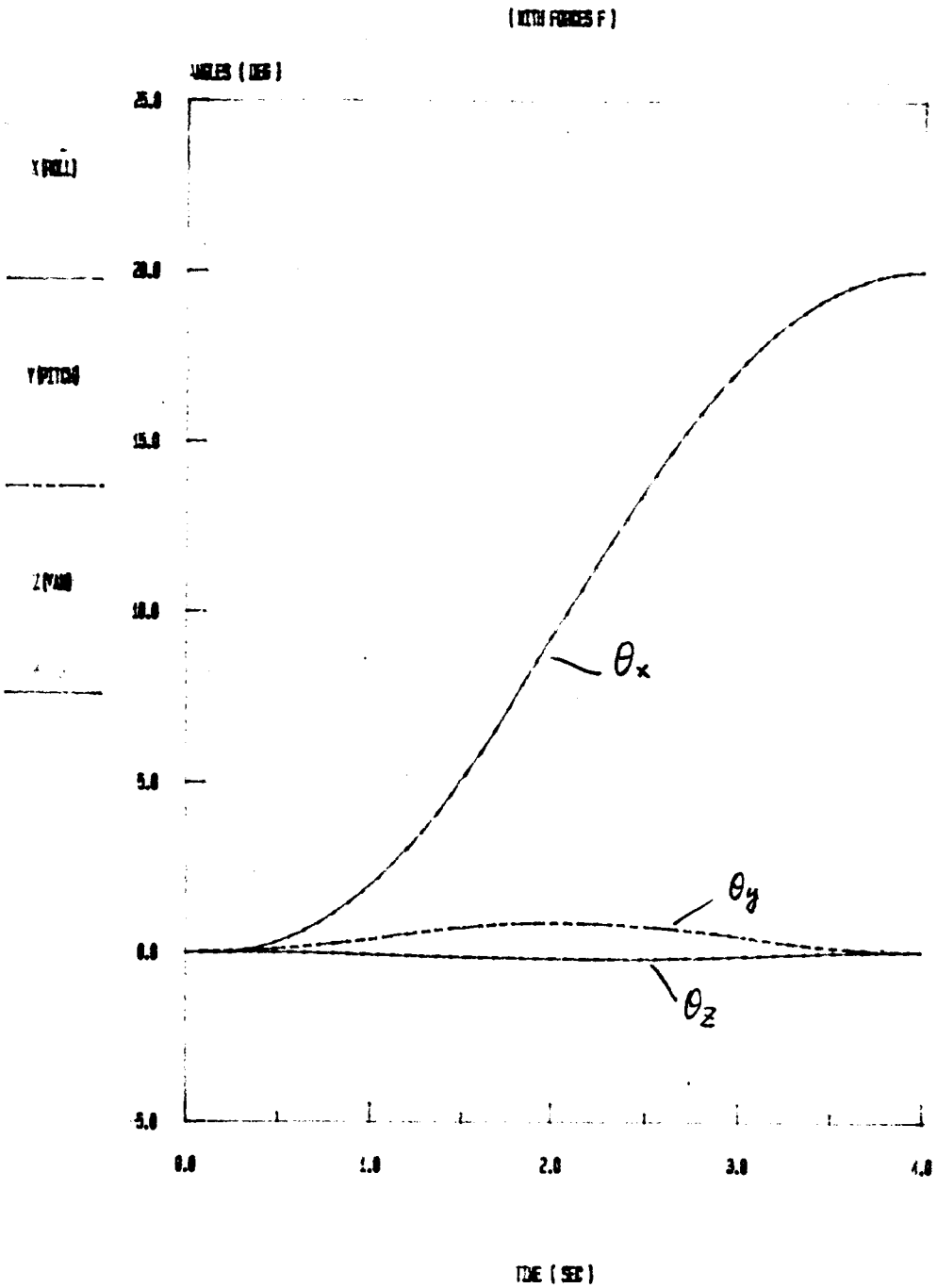

Fig. 9a CONTROL TORQUES (Z-AXIS SLEWING)

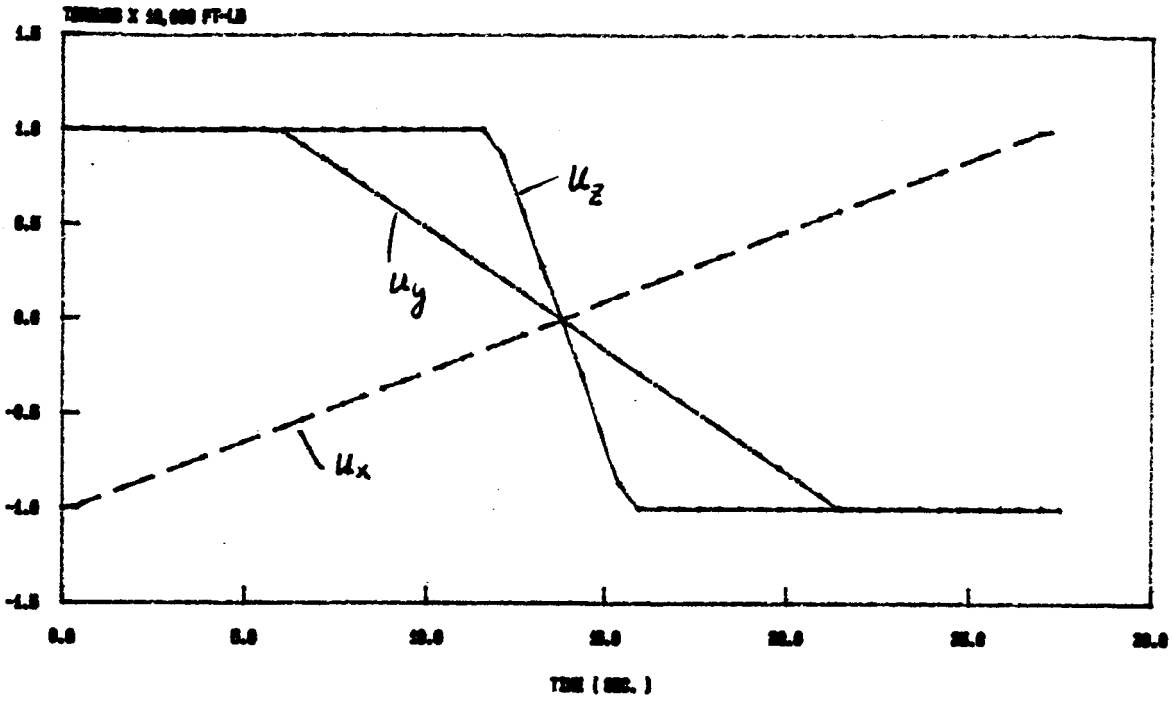

Fig. 9b CONTROL FORCES (Z-AXIS SLEWING)

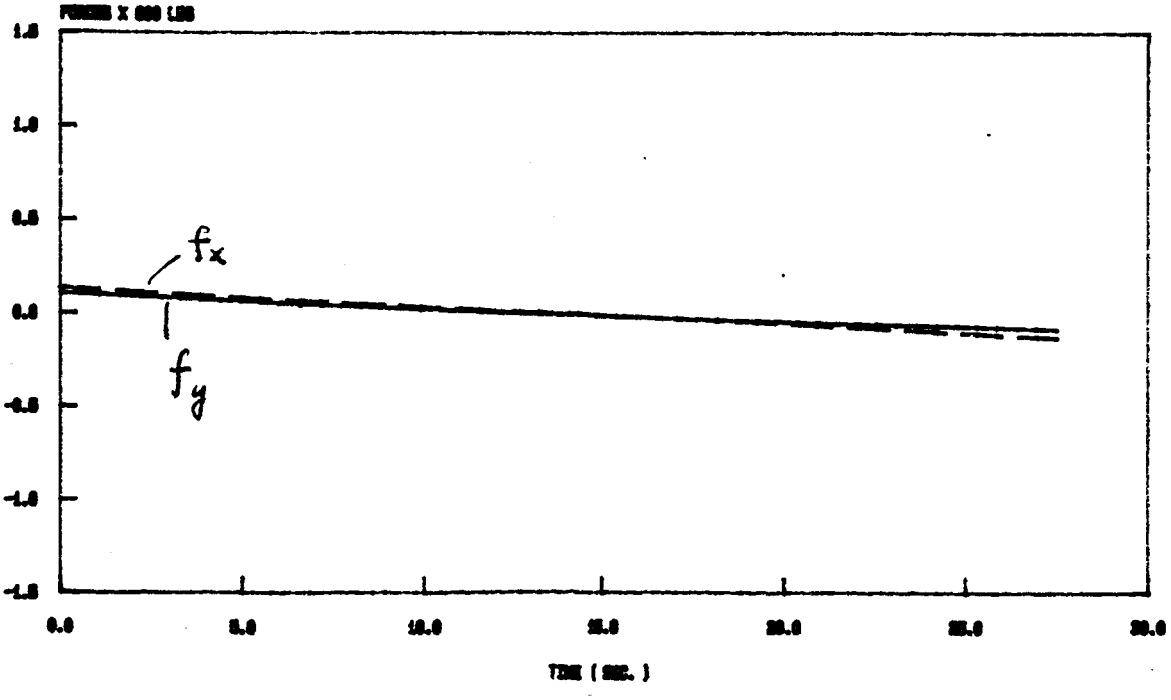

Fig. 10a CONTROL TORQUES (Z-AXIS SLEWING)

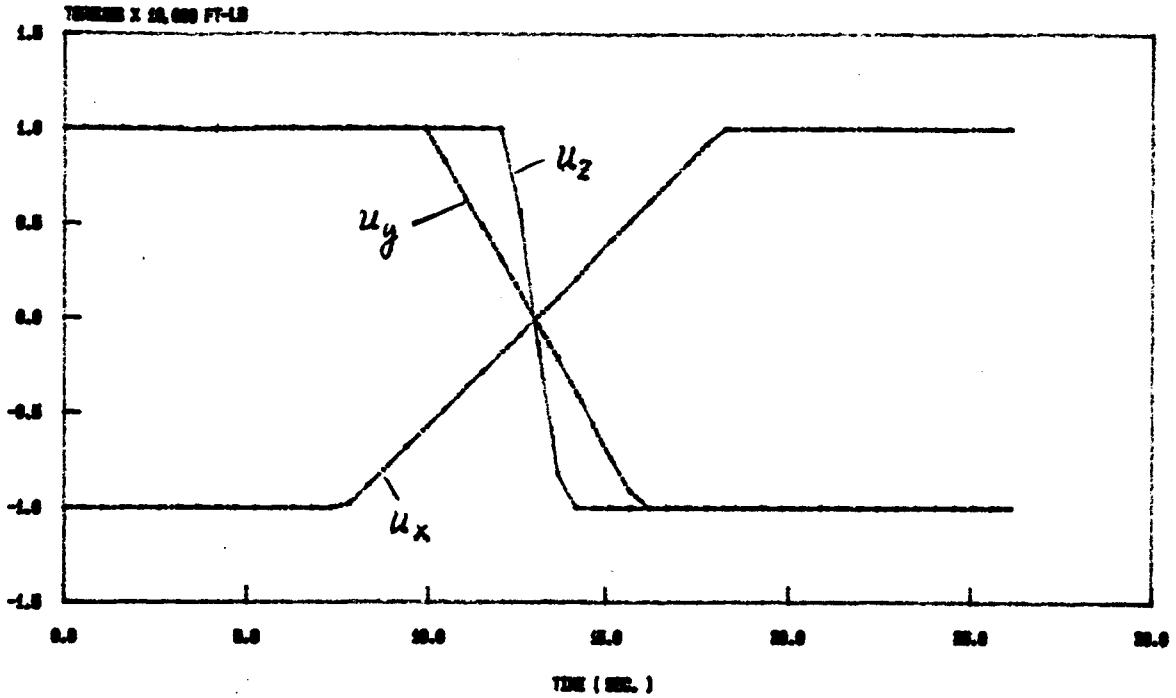

Fig. 10b CONTROL FORCES (Z-AXIS SLEWING)

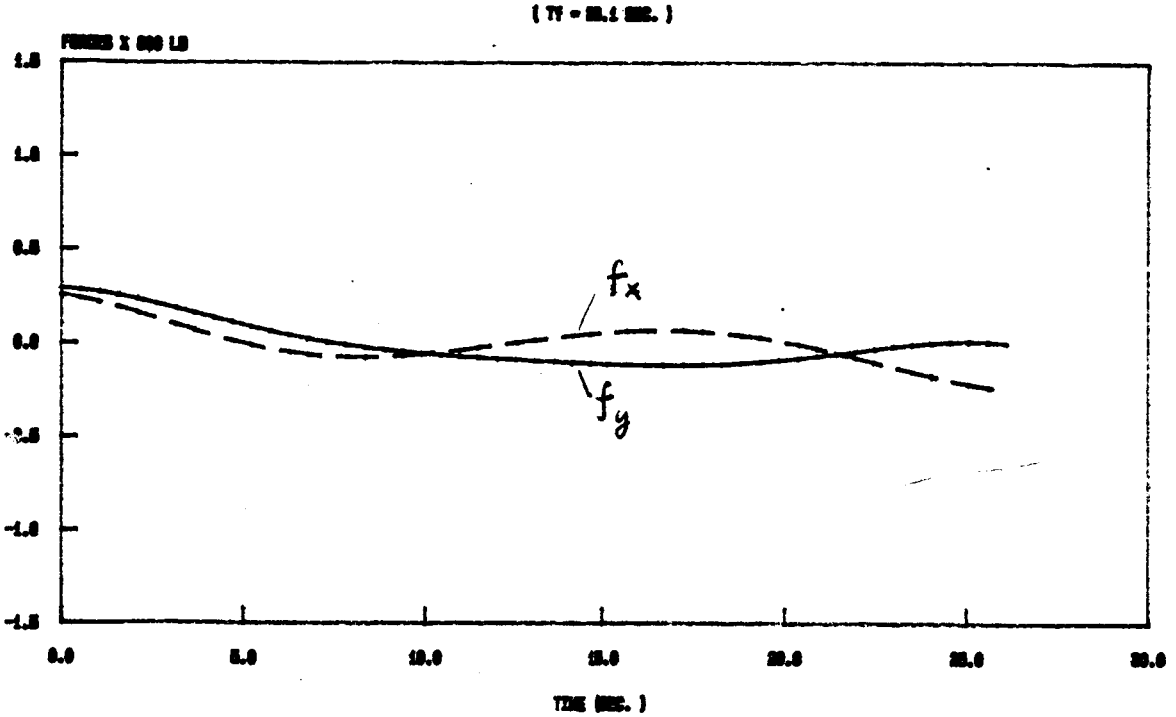

Fig. 11a CONTROL TORQUES (Z-AXIS SLEWING)

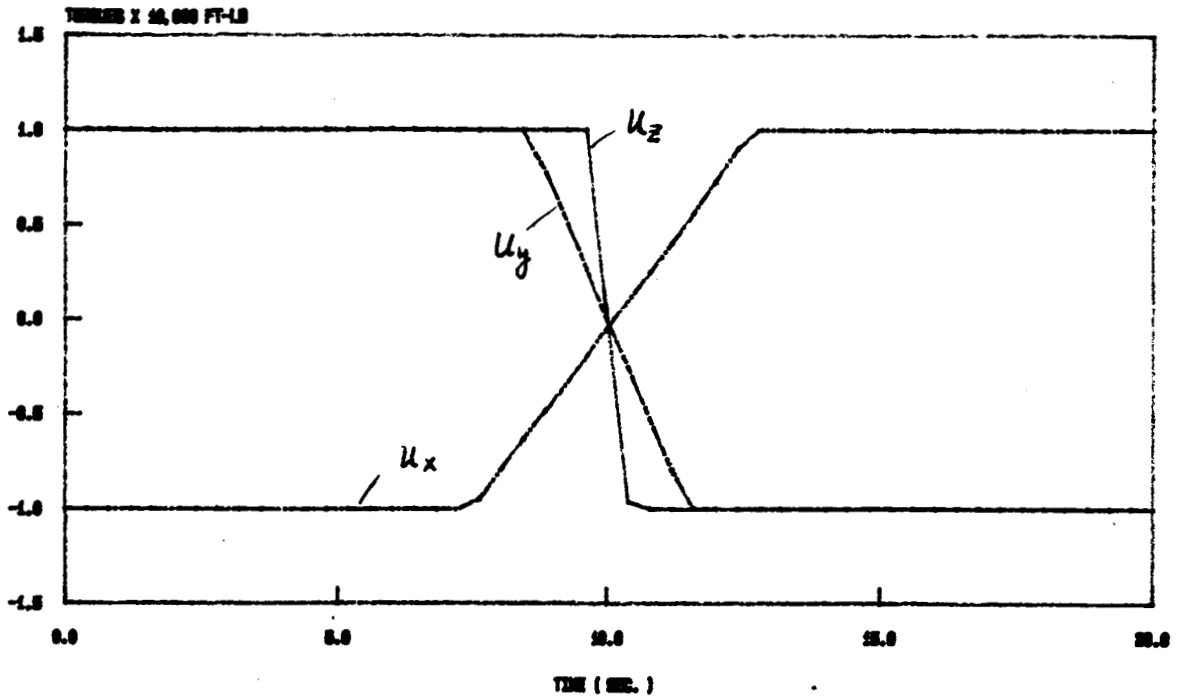

Fig. 11b CONTROL FORCES (Z-AXIS SLEWING)

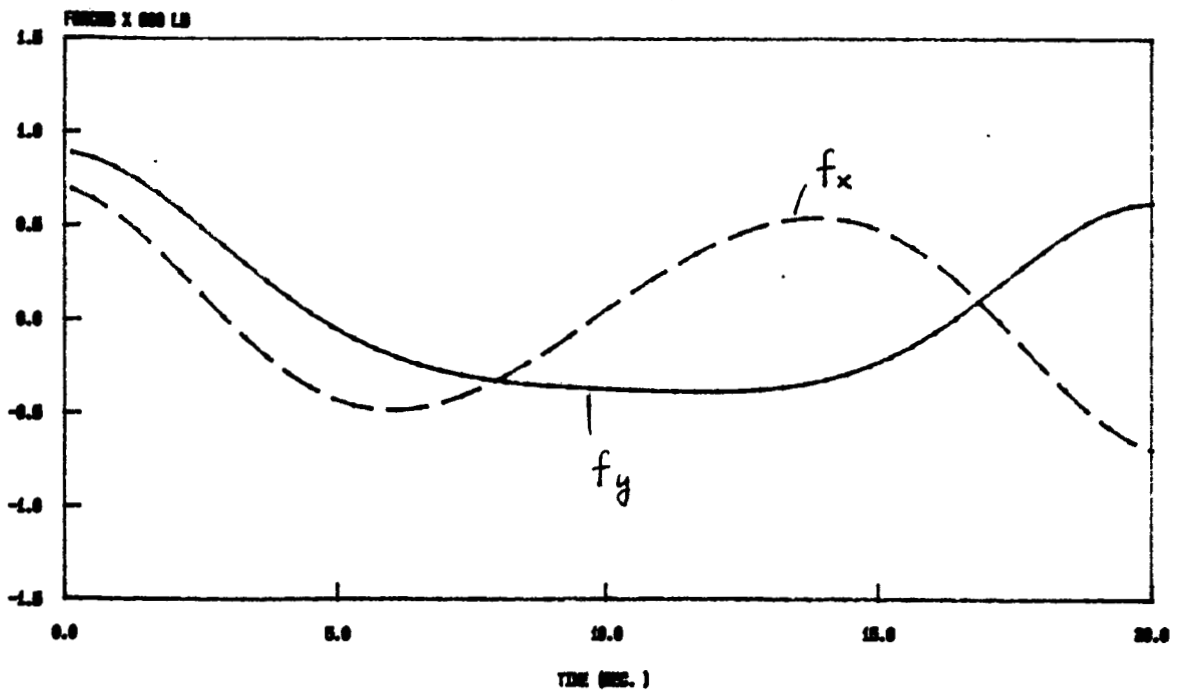

Fig. 12 ATTITUDE ANGLES (Z-AXIS SLEWING)

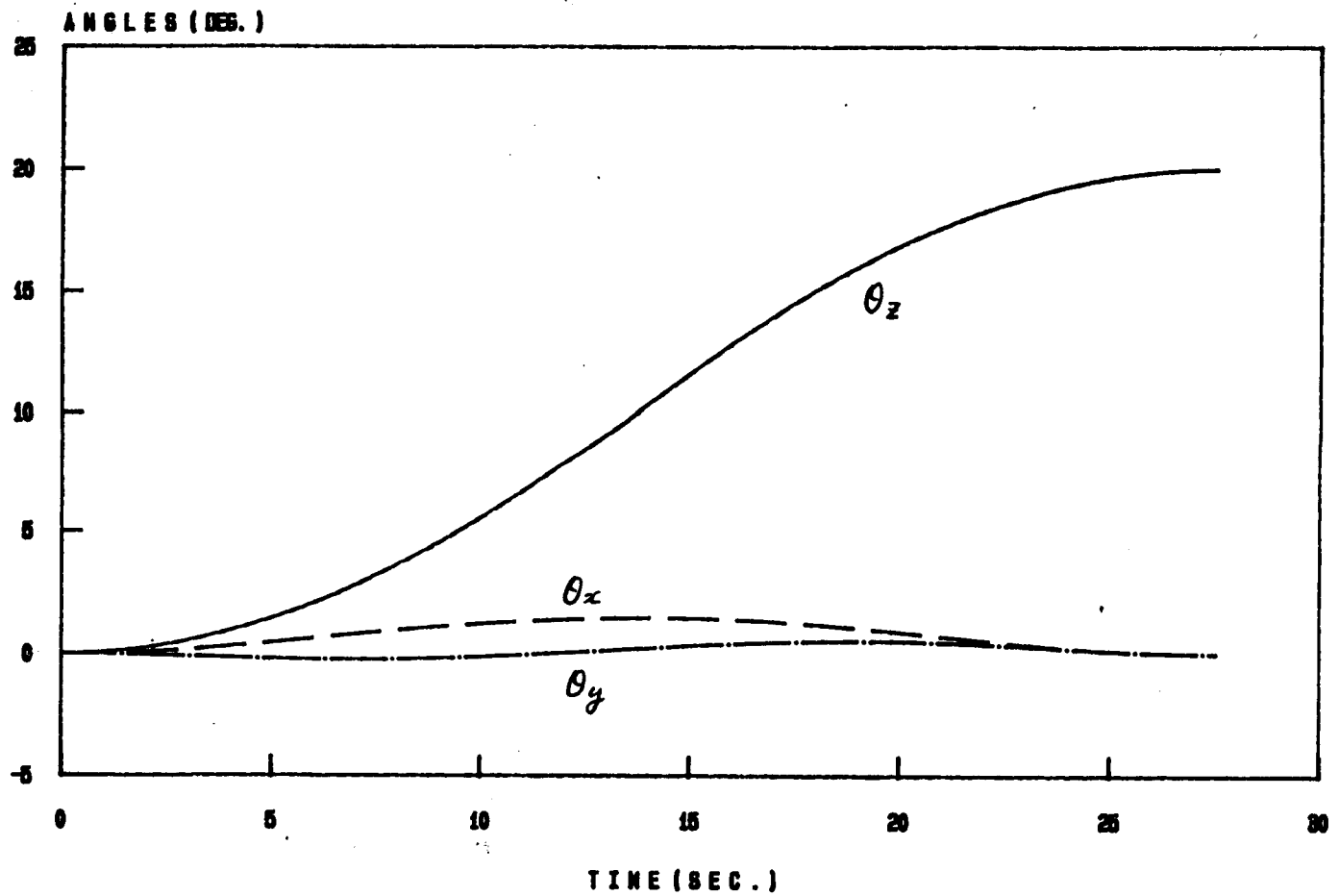

Fig. 13 ATTITUDE ANGLES (Z-AXIS SLEWING)

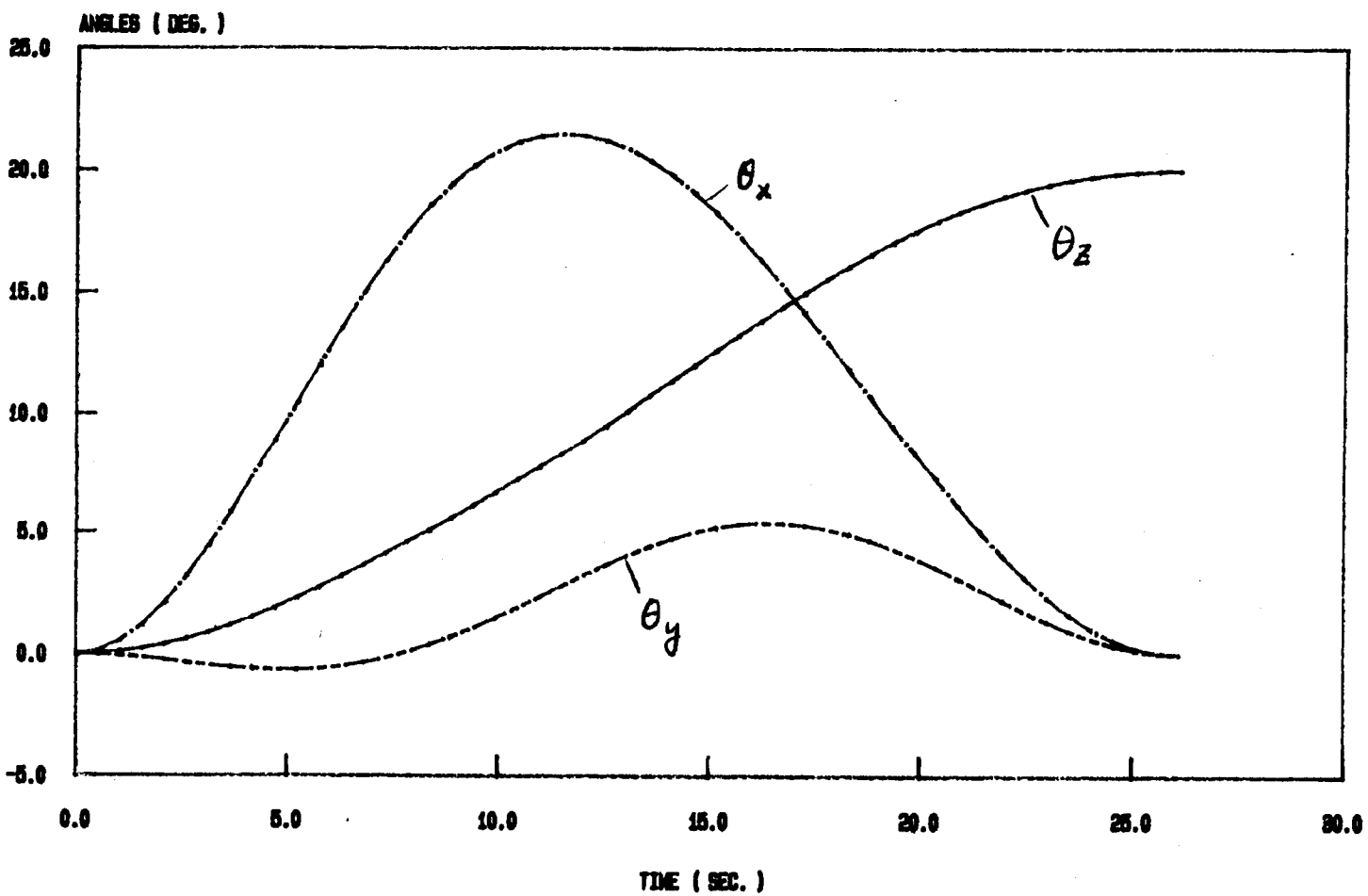

Fig. 14 ATTITUDE ANGLES (Z-AXIS SLEWING)

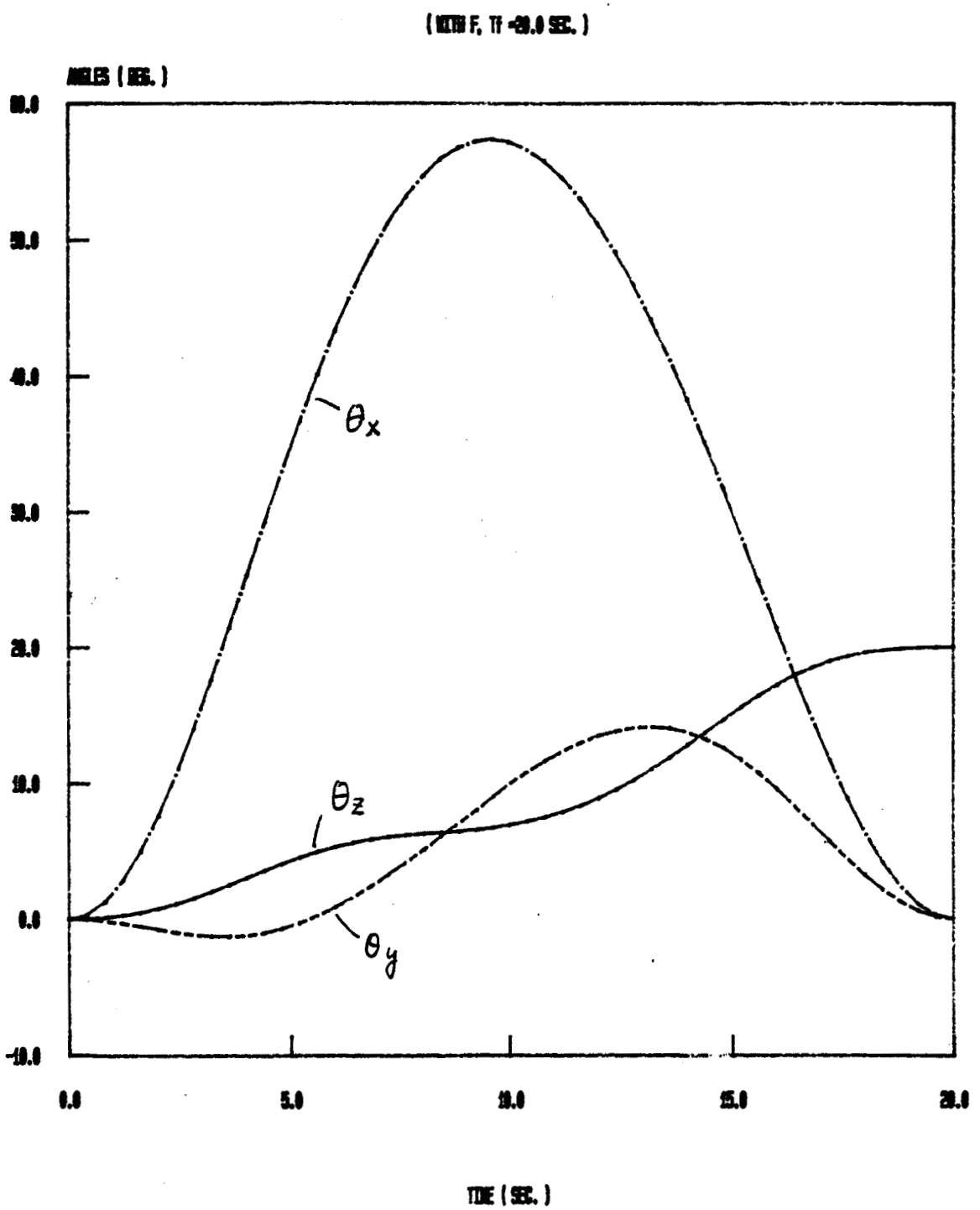

Fig. 15a CONTROL TORQUES U (SCOLE--EXAMPLE)

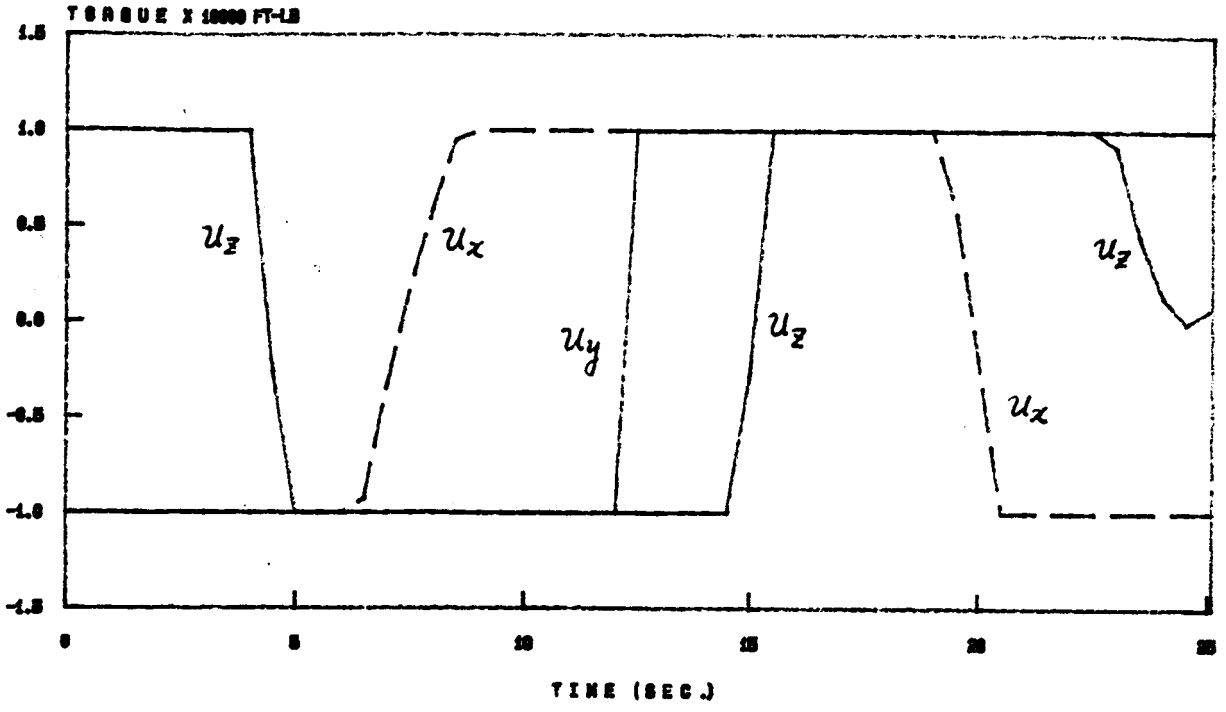

Fig. 15b ATTITUDE ANGLES (SCOLE--EXAMPLE)

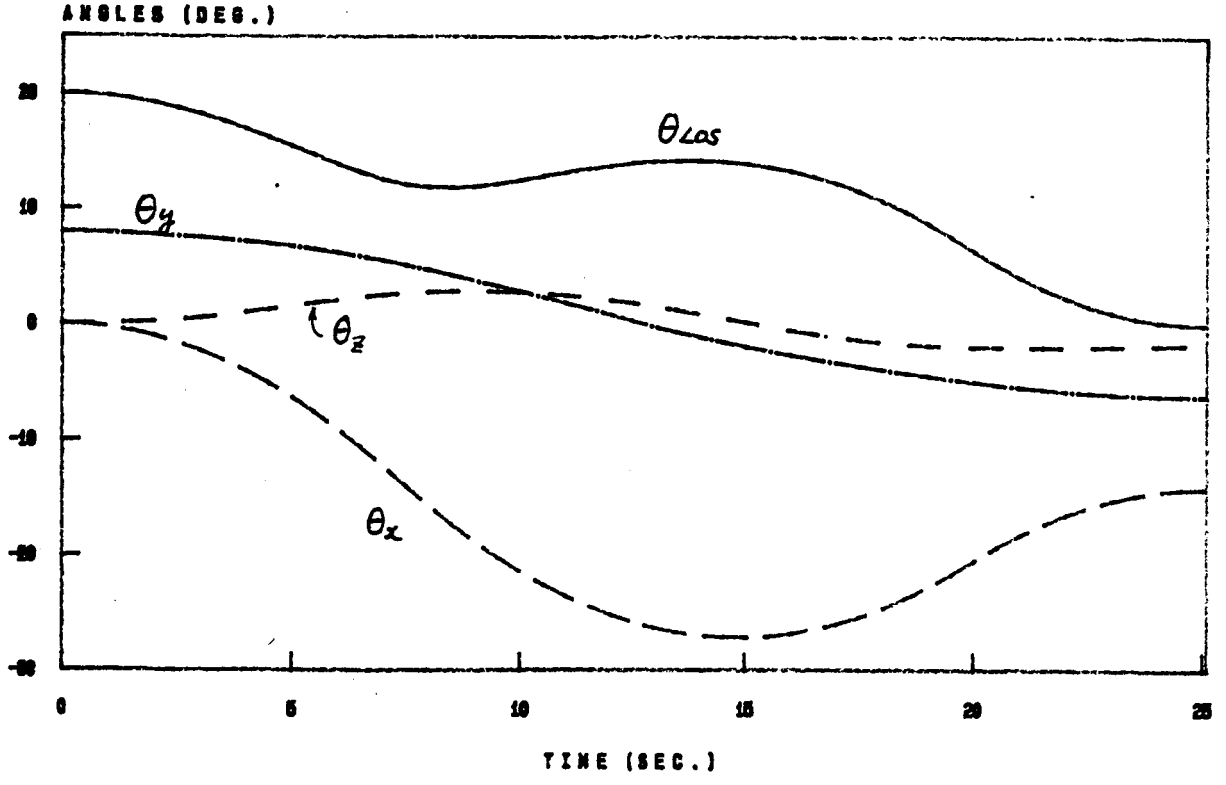

Appendix I The term $g(\omega, r)$ in Eq.(16)

The term $I^{-1}\tilde{\omega} I \omega$ in dynamical equation (9) can be replaced by

$$I^{-1}\tilde{\omega} I \omega = \left[\begin{array}{ccc:ccc} a_{11} & a_{12} & a_{13} & b_{11} & b_{12} & b_{13} \\ a_{21} & a_{22} & a_{23} & b_{21} & b_{22} & b_{23} \\ a_{31} & a_{32} & a_{33} & b_{31} & b_{32} & b_{33} \end{array}\right] \begin{bmatrix} \omega_1^2 \\ \omega_1^2 \\ \omega_1^2 \\ \omega_2\,\omega_3 \\ \omega_3\,\omega_1 \\ \omega_1\,\omega_2 \end{bmatrix}$$

$$= [\ A\ :\ B\ ]\ \bar{\bar{\omega}}$$

where the a_{ij} and b_{ij} (the elements of matrices A and B) are constants associated with the inertia parameters of the spacecraft.

Then the term $r^T I^{-1}\tilde{\omega} I \omega$ of the Hamiltonian, H, in Eq.(14) has the form

$$h = r^T I^{-1}\tilde{\omega} I \omega = [\ r_1\ r_2\ r_3\ ][\ A\ :\ B\ ]\ \bar{\bar{\omega}}$$
$$= R_1\omega_1^2 + R_2\omega_2^2 + R_3\omega_3^2 + R_4\omega_2\omega_3 + R_5\omega_3\omega_1 + R_6\omega_1\omega_2$$

where R_i are the linear combinations of r_j

$$\begin{bmatrix} R_1 \\ R_2 \\ R_3 \end{bmatrix} = A^T r \quad ; \qquad \begin{bmatrix} R_4 \\ R_5 \\ R_6 \end{bmatrix} = B^T r$$

The term $g(\omega, r)$ in Eq.(16) is obtained by

$$g(\omega, r) = -\frac{\partial h}{\partial \omega} = - \begin{bmatrix} 2R_1 & R_6 & R_5 \\ R_6 & 2R_2 & R_4 \\ R_5 & R_4 & 2R_3 \end{bmatrix} \begin{bmatrix} \omega_1 \\ \omega_2 \\ \omega_3 \end{bmatrix}$$

Appendix II Solution of Eq.(44)

Eq. (44) can be rewritten as

$$a_i \ddot{\theta} = b_i \dot{\theta}^2 + c_i \tau_i \qquad (44)$$

For simplicity, we only consider the solutions for the following boundary conditions

$$\theta(0)=0, \quad \dot{\theta}(0)=0 \qquad (II\text{-}1)$$

$$\theta(t_f)=\theta^*, \quad \dot{\theta}(t_f)=0 \qquad (II\text{-}2)$$

Suppose $a_i \neq 0$, and let

$$b = b_i/a_i , \qquad c = c_i/a_i$$

we can rewrite Eq.(44) as

$$\ddot{\theta} = b \dot{\theta}^2 + c \tau \qquad (II\text{-}3)$$

where we also suppose $c>0$.

Since the control for this problem is of a bang-bang type with only one switching point, then, for $\tau=+1$,

$$\ddot{\theta} = b \dot{\theta}^2 + c \qquad (II\text{-}4)$$

By integrating Eq.(II-4) and using condition (II-1), we can get

$$\dot{\theta} = \sqrt{(c/b)(e^{2b\theta} - 1)} \qquad (II\text{-}5)$$

For $\tau=-1$,

$$\ddot{\theta} = b \dot{\theta}^2 - c \qquad (II\text{-}6)$$

By integrating Eq.(II-6) and using condition (II-2),

$$\dot{\theta} = \sqrt{(c/b)(1 - e^{2b(\theta-\theta^*)})} \qquad (II\text{-}7)$$

By equating Eqs. (II-5) and (II-7), we get $\theta=\theta_s$ and $\dot{\theta}=\dot{\theta}_s$ at the switching point, $t=t_s$,

$$\theta_s = \frac{1}{2b} \log \frac{2}{1+e^{-2b\theta^*}} \qquad (II\text{-}8)$$

$$\dot{\theta}_s = \sqrt{(c/b)(e^{2b\theta_s} - 1)} \qquad (II\text{-}9)$$

By integrating (II-5), we get

$$t_s = \begin{cases} \dfrac{1}{\sqrt{-bc}} \cosh^{-1}(e^{-b\theta_s}) , & b<0 ; \\ \\ \dfrac{1}{\sqrt{bc}} \left[\dfrac{\pi}{2} - \sin^{-1}(e^{-b\theta_s})\right] , & b>0 \end{cases} \qquad \text{(II-10)}$$

and by integrating Eq.(II-7), we get

$$t_f = \begin{cases} t_s + \dfrac{1}{\sqrt{-bc}} \left[\dfrac{\pi}{2} - \sin^{-1}(e^{b(\theta^*-\theta_s)})\right] , & b<0; \\ \\ t_s + \dfrac{1}{\sqrt{bc}} \cosh^{-1}[e^{b(\theta^*-\theta_s)}] , & b>0 \end{cases} \qquad \text{(II-11)}$$

For the case

$$\dot{\theta}(0) \neq 0$$

more complicated solutions can be obtained, but are not given here.

IV. CONCLUSIONS AND RECOMMENDATIONS

For large ordered systems, typical of mathematical models of proposed large space structural systems, a finite amount of time will be required to evaluate and process the control signals. These input time delays may cause instability in the closed loop systems for which the control laws were previously designed without considering the effect of the delay. It is seen that such instabilities may result even for delays that are only a small fraction of the system's fundamental open-loop period. From this study it is also observed that even a small amount of inherent (natural) damping in the system can increase the amount of delay that can be tolerated without the system becoming unstable. The control problem with delayed input is also formulated in the discrete time domain and an analysis procedure is suggested and could provide the basis for future study.

Pontryagin's maximum principle from optimal control theory has been applied to formulate slewing control strategies for a general rigid asymmetrical spacecraft system. The slewing motion need not be restricted to a single-axis maneuver and the final attitude error after the slew can be made arbitrarily small. The control effort and minimum slewing time are calculated based on a quasi-linearization algorithm for the resulting two-point boundary value problem. Euler's eigenaxis rotation theorem is used to obtain a nominal trajectory of the attitude slewing motion which is used to determine the initial (guessed) co-state values for the algorithm. Numerical examples based on the rigidized, in-orbit model of the SCOLE also include the more general reflector line-of-sight slewing maneuvers.

The guessed initial values for the co-states are sufficient to arrive at the (converged) values supplied by the algorithm. The methods used here may be implemented for practical control sources which may have more constraints. For example, in the neighborhood of the bang-bang control switching points, the jump can be replaced by a linear function of time. The control profiles obtained provide a reference for future use. An extension to the minimum time slewing motion of the SCOLE model containing both rigid and flexible components is planned.